

A new evaluation of the HZZ coupling: direct bounds on anomalous contributions and CP violating effects via a new asymmetry

A. I. Hernández-Juárez*,¹ A. Fernández-Téllez,¹ and G. Tavares-Velasco¹

¹*Facultad de Ciencias Físico Matemáticas, Benemérita Universidad Autónoma de Puebla, Apartado Postal 1152, Puebla, Puebla, México**

(Dated: March 24, 2023)

The standard model (SM) one-loop contributions to the most general $H^*Z^*Z^*$ coupling are obtained via the background field method in terms of Passarino-Veltman scalar functions, from which the contributions to the H^*ZZ and HZZ^* couplings are obtained in terms of two CP -conserving $h_{1,2}^V$ and one CP -violating h_3^V form factors ($V = H, Z$). The current CMS constraints on the HZZ coupling ratios are then used to obtain bounds on the real part of the anomalous HZZ couplings, which are up to two orders of magnitude tighter than previous ones, and also on the corresponding absorptive parts, which are the first one of this kind. The effects of the absorptive parts of the HZZ anomalous couplings, which have been overlooked in the past, are analyzed via the partial decay width $\Gamma_{H^* \rightarrow ZZ}$, and a significant deviation from the SM tree-level contribution is observed at low energies, though it becomes negligible at high energies. We also explore the possibility that polarized Z gauge bosons are used for the study of non-SM couplings via a new left-right asymmetry \mathcal{A}_{LR} , which is sensitive to CP -violating complex form factors and can be as large as the unity at best, and in a more conservative scenario it is still larger by five or four orders of magnitude than the SM prediction arising until the three-loop level. The partial decay widths $\Gamma_{H^* \rightarrow Z_L Z_L}$ and $\Gamma_{H^* \rightarrow Z_R Z_R}$ are also studied in several scenarios and it is observed that the deviations from the SM results can be large at high energies and in this case, increases as the energy increases. Thus the use of polarized Z gauge bosons could give hints of CP violation.

I. INTRODUCTION

The observation of the Higgs boson at the CERN LHC [1, 2] was clear evidence that the mechanism of electroweak gauge symmetry breaking is realized in nature as conjectured by the Glashow-Weinberg-Salam Standard Model (SM) of elementary particles. Up to now, the data collected at the LHC has confirmed that the properties of the Higgs particle are consistent with the SM predictions, though some of its couplings are yet to be measured, such as those to light fermions and its self-couplings as well. It is expected that the LHC Run 3 can also explore hints of some anomalous Higgs couplings. Along these lines, the CMS collaboration has reported for the first time data on the off-shell H^*ZZ coupling via off-shell Higgs boson production (O-SHBP) $pp \rightarrow H^* \rightarrow ZZ$ [3], which requires that the four-momentum of the off-shell Higgs boson is above the threshold $||q|| = 2m_Z$. According to the SM, 10% of V pair production events at the LHC are due to the H^*VV coupling [4], which is statistically large enough to allow measurement. Moreover, it has been found that the VV invariant mass kinematic distribution is sensitive to the off-shell H^*ZZ contribution, whereas the ratio of off-shell to on-shell production rates can be used to determine the Higgs decay width Γ_H [5, 6].

The phenomenological and experimental implications of the H^*ZZ coupling at the LHC and future colliders have been explored in the past and also very recently [7–15]. Furthermore, the off-shell HZZ^* coupling has several phenomenological implications, which have been studied through HZ production [16–34]. Thus, the HZZ coupling is worth studying, thereby requiring a highly precise determination of all its lowest-order contributions. In particular, the search for any anomalous contribution to the H^*ZZ coupling will play an important role in the LHC program soon.

Off-shell couplings have been of great interest in recent years [35–37] as they can develop an imaginary (absorptive) part due to the optical theorem, thereby giving rise to some effects on physical processes. The absorptive part of a coupling has already been studied for instance in the off-shell chromomagnetic and chromoelectric dipole moments of quarks [38, 39] and also in the trilinear neutral gauge boson couplings [40, 41], which requires that at least one of the three gauge bosons is off-shell to be non-vanishing [42, 43]. Also, the phenomenological implications of the absorptive part of the off-shell Higgs boson coupling H^*ZZ have been brought to attention by many authors [18, 20, 22, 28], nonetheless, to our knowledge, a precise determination of the SM contribution has not been reported yet, which may stem from the fact that there has been some controversy on whether or not off-shell couplings represent valid

* alaban7_3@hotmail.com

observable quantities. We will dwell on this issue below. In particular, the study of the absorptive part of the H^*ZZ and HZZ^* couplings may be relevant at the LHC and future colliders as it can explain slight deviations on some physical observables. Such as the case for the absorptive part of the ttg coupling, which has direct effects on top pair production at the LHC [37].

The one-loop corrections to the HZZ coupling were calculated long ago in the SM [44, 45] and also recently [46]. On the other hand, the new physics contributions have also been reported in several beyond SM theories, such as the two-Higgs doublet model [47], the minimal Higgs triplet model (HTM) [48], the Higgs singlet model (HSM) [47] and the minimal supersymmetric standard model (MSSM) [36]. Nevertheless, some of those results are reported in a somewhat old-fashioned notation, which can lead to some confusion when a numerical calculation is worked out and a cross-check is required. Therefore, a new evaluation of the SM one-loop contributions to the off-shell H^*ZZ coupling with a more up-to-date notation for the analytical results is in order. The purpose of this work is to present such an evaluation. Afterward, we will use our analytical results and the current LHC data to obtain limits on the real and absorptive parts of the anomalous couplings of the HZZ vertex. These new bounds can be relevant because of the O-SHBP results. Furthermore, their implications may be observed in the Z boson pair production.

The rest of this work is organized as follows. In Section II we analyze the most general effective Lagrangian for the HZZ coupling up to dimension-five operators, along with the most popular parametrizations used to study the effects of this coupling at particle colliders. Sec. III is devoted to describing the calculation of the SM one-loop contributions to the off-shell H^*ZZ and HZZ^* couplings via the background field method, which in the Feynman-t'Hooft gauge yields identical results to those obtained via the Pinch technique. This method is known to give gauge-independent and finite off-shell Green's functions. The analytical results are presented in Appendix A in terms of Passarino-Veltman scalar functions. In Section IV we present the numerical analysis of the behavior of the H^*ZZ and HZZ^* couplings as functions of the off-shell boson transfer momentum and we also obtain bounds on the anomalous terms of such couplings, which are used in Sec. VI to study the Z pair production off an off-shell Higgs boson, for which we introduce a new asymmetry defined for polarized Z bosons. Finally, in Section VII we present the conclusions and outlook.

II. THEORETICAL FRAMEWORK

Several parametrizations have been introduced in the literature to study the phenomenology of the HZZ coupling. It is thus worth presenting an overview of them with the aim that our analysis can be straightforwardly compared with similar studies. The effective Lagrangian up to dimension-five operators for the HZZ interaction can be written in the so-called Hagiwara basis [17, 18, 23] as follows

$$\mathcal{L} = \frac{g}{c_W} m_Z \left[\frac{(1 - a_Z)}{2} H Z_\mu Z^\mu + \frac{1}{2m_Z^2} \left\{ b_Z H Z_{\mu\nu} Z^{\mu\nu} + c_Z \left((\partial_\mu H) Z_\nu - (\partial_\nu H) Z_\mu \right) Z^{\mu\nu} + \tilde{b}_Z H Z_{\mu\nu} \tilde{Z}^{\mu\nu} \right\} \right], \quad (1)$$

where $Z_{\mu\nu} = \partial_\mu Z_\nu - \partial_\nu Z_\mu$ and $\tilde{Z}_{\mu\nu} = \epsilon_{\mu\nu\alpha\beta} Z^{\alpha\beta}/2$. In the SM a_Z vanishes at the tree level, the CP conserving form factors b_Z and c_Z are induced up to one-loop level [45], and the CP violating form factor \tilde{b}_Z arises up to the three-loop level [7] and has been estimated to be of the order of 10^{-11} [49]. The b_Z , c_Z and \tilde{b}_Z form factors are absent at the tree level in the SM but can receive anomalous contributions from new physics at the one-loop-level or higher orders of perturbation theory. In Fig. 1, we introduce the notation used throughout the rest of this work for the vertex function $\Gamma_{\mu\nu}^{ZZH}$.

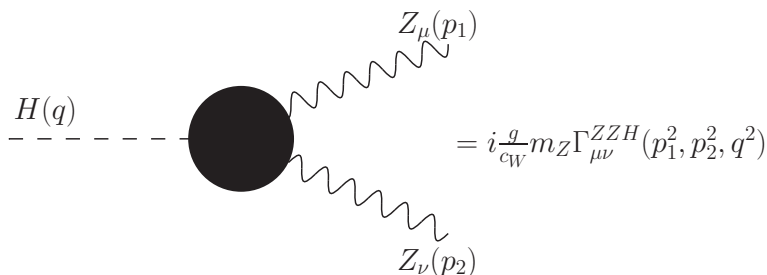


FIG. 1. Nomenclature for the HZZ coupling and the $\Gamma_{\mu\nu}^{ZZH}$ vertex function.

Although we are mainly interested in processes where there is an off-shell Higgs boson as in the H^*ZZ coupling, for completeness we will also study the case of the HZZ^* coupling, which has been widely studied as it has several

implications at particle colliders [16–33]. Therefore, in the Lagrangian of (1), we neglect the scalar component of the Z gauge bosons by setting $\partial_\mu Z^\mu = 0$ and consider the kinematics $H^* \rightarrow ZZ (Z^* \rightarrow HZ)$ along with the notation of Fig. 1 to obtain the vertex function for both the Higgs boson and one Z gauge boson are off-shell:

$$\Gamma_{\mu\nu}^{ZZH} = h_1^V(q^2, p_1^2, p_2^2)g_{\mu\nu} + \frac{h_2^V(q^2, p_1^2, p_2^2)}{m_Z^2}p_{1\nu}p_{2\mu} + \frac{h_3^V(q^2, p_1^2, p_2^2)}{m_Z^2}\epsilon_{\mu\nu\alpha\beta}p_1^\alpha p_2^\beta, \quad (2)$$

where V stands for the off-shell boson and the dependence of the h_i^V form factors have been written explicitly. The relation between the form factors h_i and the parameters of Lagrangian (1) for the kinematics $H^* \rightarrow ZZ (Z^* \rightarrow HZ)$ are

$$h_1^V(q^2, p_1^2, p_2^2) = 1 + a_Z - b_Z \frac{q^2 - p_1^2 - p_2^2}{m_Z^2} + c_Z \frac{q^2}{m_Z^2}, \quad (3)$$

$$h_2^V(q^2, p_1^2, p_2^2) = \pm 2(b_Z - c_Z), \quad (4)$$

$$h_3^V(q^2, p_1^2, p_2^2) = \pm 2\tilde{b}_Z. \quad (5)$$

For $V = H$ ($V = Z$) the Z (H) boson is on-shell, and we have $p_1^2 = m_Z^2$ ($q^2 = m_H^2$), whereas for both cases $p_2^2 = m_Z^2$. The structure of Eq. (2) is the same for three, two, or one off-shell bosons provided that one assumes that the Z gauge bosons are coupled to conserved currents. It is worth noticing that the basis used in the Lagrangian (1) is not unique. From the equations of motion, one has

$$HZ_\mu \partial_\nu Z^{\mu\nu} = \frac{1}{2} \left((\partial_\mu H) Z_\nu - (\partial_\nu H) Z_\mu \right) Z^{\mu\nu} + \frac{1}{2} Z_{\mu\nu} Z^{\mu\nu}, \quad (6)$$

where a surface term has been dropped. Thus the HZZ coupling can be alternatively written as

$$\mathcal{L} = \frac{g}{c_W} m_Z \left[\frac{(1 - a_Z)}{2} H Z_\mu Z^\mu + \frac{1}{2m_Z^2} \left\{ \hat{b}_Z H Z_{\mu\nu} Z^{\mu\nu} + \hat{c}_Z H Z_\mu \partial_\nu Z^{\mu\nu} + \tilde{b}_Z H Z_{\mu\nu} \tilde{Z}^{\mu\nu} \right\} \right], \quad (7)$$

where the \hat{b}_Z and \hat{c}_Z form factors are given as $\hat{b}_Z = b_Z - c_Z$ and $\hat{c}_Z = 2c_Z$. In this notation, the form factors h_i^V of Eq. (2) are now given by

$$h_1(q^2, p_1^2, p_2^2) = 1 + a_Z - \hat{b}_Z \frac{q^2 - p_1^2 - p_2^2}{m_Z^2} + \frac{\hat{c}_Z}{2} \frac{p_1^2 + p_2^2}{m_Z^2}, \quad (8)$$

$$h_2(q^2, p_1^2, p_2^2) = \pm 2\hat{b}_Z, \quad (9)$$

$$h_3(q^2, p_1^2, p_2^2) = \pm 2\tilde{b}_Z. \quad (10)$$

The main difference between the basis of Lagrangians (1) and (7) is that the form factor h_2^V is given in terms of only one parameter in (7). Although one could find analytic expressions for each h_i^V in a particular theory, it would not be possible to extract the partial contribution from b_Z and c_Z . Also, it turns out that both parametrizations are used without any distinction in the literature, which may be confusing for a cross-check of the numerical results. Thus, to avoid a misleading analysis of the HZZ coupling, we present our results in terms of the parametrization in Lagrangian (7). It is more suited for this work as we can calculate the form factor h_2 and then extract the exact SM contribution to the \hat{b}_Z coefficient.

Direct bounds on the HZZ anomalous couplings have been obtained using polarization observables of the Z gauge boson produced via the $Z^* \rightarrow HZ$ coupling at the LHC at $\sqrt{s} = 14$ TeV [28]. According to the notation of Lagrangian (7) such bounds read

$$|\text{Re}[\hat{b}_Z]| \leq 3.5 \times 10^{-4}, \quad |\text{Im}[\hat{b}_Z]| \leq 7.94 \times 10^{-3}, \quad (11)$$

$$|\text{Re}[\tilde{b}_Z]| \leq 4.76 \times 10^{-3}, \quad |\text{Im}[\tilde{b}_Z]| \leq 6.64 \times 10^{-3}, \quad (12)$$

Other limits on the anomalous HZZ couplings have been obtained from the analysis of several processes at e^+e^- [18, 23], ep [25] and γe colliders [9]. Below we will discuss some parametrizations used by several authors in the study of the HZZ coupling and their relationship with the above parametrizations.

A. The LHC framework

In the analysis of the CMS collaboration, the following parametrization is used for the scattering amplitude of the process where the H^*ZZ interaction is involved [50]

$$A(H \rightarrow ZZ) \sim \frac{1}{v} \left[a_1^{ZZ} + \frac{\kappa_1^{ZZ} p_1^2 + \kappa_2^{ZZ} p_2^2}{(\Lambda_1^{ZZ})^2} \right] m_Z^2 \epsilon_1^* \epsilon_2^* + \frac{a_2^{ZZ}}{v} f_{\mu\nu}^{*(1)} f^{*(2)\mu\nu} + \frac{a_3^{ZZ}}{v} f_{\mu\nu}^{*(1)} \tilde{f}^{*(2)\mu\nu}, \quad (13)$$

where we use the notation of Fig. 1. Also $f^{(i)\mu\nu} = \epsilon_i^\mu p_i^\nu - \epsilon_i^\nu p_i^\mu$ and $\tilde{f}^{(i)} = \epsilon_{\mu\nu\rho\sigma} f^{(i)\rho\sigma}$ are the field and dual field strength tensors of the Z_i gauge boson with polarization vector ϵ_i and four-momentum p_i . In the SM $a_1^{ZZ} = 2$ at the tree level. We can rewrite the above expression in terms of the h_i^V form factors. In the Hagiwara basis (1) and using the kinematics for $H^* \rightarrow ZZ$ we find the following relations:

$$h_1(q^2, p_1^2, m_Z^2) = \frac{a_1^{ZZ}}{2} + \frac{\kappa_1^{ZZ} p_1^2 + \kappa_2^{ZZ} p_2^2}{2(\Lambda_1^{ZZ})^2} + \frac{a_2^{ZZ}}{2} \frac{q^2 - p_1^2 - p_2^2}{m_Z^2}, \quad (14)$$

$$h_2(q^2, p_1^2, m_Z^2) = -a_2^{ZZ}, \quad (15)$$

$$h_3(q^2, p_1^2, m_Z^2) = -a_3^{ZZ}. \quad (16)$$

Thus, we can identify

$$1 + a_Z = \frac{a_1^{ZZ}}{2}, \quad (17)$$

$$-b_Z \frac{q^2 - p_1^2 - p_2^2}{m_Z^2} + c_Z \frac{q^2}{m_Z^2} = \frac{\kappa_1^{ZZ} p_1^2 + \kappa_2^{ZZ} p_2^2}{2(\Lambda_1^{ZZ})^2} + \frac{a_2^{ZZ}}{2} \frac{q^2 - p_1^2 - p_2^2}{m_Z^2}, \quad (18)$$

$$b_Z - c_Z = -\frac{a_2^{ZZ}}{2}, \quad (19)$$

$$\tilde{b}_Z = -\frac{a_3^{ZZ}}{2}, \quad (20)$$

which yields the following relationship

$$c_Z \frac{p_1^2 + p_2^2}{m_Z^2} = \frac{\kappa_1^{ZZ} p_1^2 + \kappa_2^{ZZ} p_2^2}{2(\Lambda_1^{ZZ})^2}, \quad (21)$$

for the case of $\kappa_1^{ZZ} = \kappa_2^{ZZ}$ and $\Lambda_1^{ZZ} \equiv m_Z$ gives

$$c_Z = \frac{\kappa_1^{ZZ}}{2}. \quad (22)$$

On the other hand, in the basis of Lagrangian (7) we can identify

$$-\hat{b}_Z \frac{q^2 - p_1^2 - p_2^2}{m_Z^2} + \frac{\hat{c}_Z}{2} \frac{p_1^2 + p_2^2}{m_Z^2} = \frac{\kappa_1^{ZZ} p_1^2 + \kappa_2^{ZZ} p_2^2}{2(\Lambda_1^{ZZ})^2} + \frac{a_2^{ZZ}}{2} \frac{q^2 - p_1^2 - p_2^2}{m_Z^2} \quad (23)$$

$$\hat{b}_Z = -\frac{a_2^{ZZ}}{2}, \quad (24)$$

whereas Eqs. (17) and (20) remain valid. For $\kappa_1^{ZZ} = \kappa_2^{ZZ}$ and $\Lambda_1^{ZZ} \equiv m_Z$, we obtain

$$\hat{c}_Z = \kappa_1^{ZZ}. \quad (25)$$

Therefore, the parametrization of the H^*ZZ vertex in (13) is redundant since only one form factor k_i^{ZZ} is necessary for both bases. In the rest of this paper, we will consider the relations (17), (20), (24) and (25).

Indirect bounds on a_i^{ZZ} coefficients have been obtained by the CMS collaboration [3, 51–53] through effective fractional cross sections f_{ai} . This approach allows one to minimize the uncertainties and it is independent of the coupling parametrization. The effective cross-section ratios are defined as

$$f_{ai}^{ZZ} = \frac{|a_i^{ZZ}|^2 \alpha_{ii}^{(2e2\mu)}}{\sum_j |a_j^{ZZ}|^2 \alpha_{jj}^{(2e2\mu)}} \text{sign} \left(\frac{a_i^{ZZ}}{a_1^{ZZ}} \right), \quad (26)$$

where the coefficients $\alpha_{ii}^{(2e2\mu)}$ are the cross-sections for the processes where two lepton pairs $2e + 2\mu$ emerge from the processes $H \rightarrow Z\gamma^*/\gamma^*\gamma^* \rightarrow 2e2\mu$, for $a_i^{ZZ} = 1$. The corresponding numerical values, which can be obtained through Monte-Carlo simulation and are normalized with respect to the coefficient $\alpha_{11}^{(2e2\mu)}$, are shown in Table I. In the CMS analysis, the couplings are considered real. Therefore, the relative phase between the couplings a_i^{ZZ} is 0 or π . The current bounds from CMS [3] are shown in Table II.

TABLE I. Anomalous couplings a_i^{ZZ} , cross sections ratios f_{ai}^{ZZ} and coefficients α_{ii}/α_{11} considered in this work. We use the relationship $a_i^{ZZ} = a_i^{WW}$ and the value $\Lambda_1 = m_Z$ for the case of the κ_1^{ZZ} coupling. The negative sign arises from the convention in Eq. (26) adopted in [54].

a_i^{ZZ}	f_{ai}^{ZZ}	α_{ii}/α_{11}
a_3	f_{a3}	0.153
a_2	f_{a2}	0.361
$-k_1$	f_{Λ_1}	1.016

TABLE II. Allowed intervals at the 95% CL for the coupling parameters f_{ai} obtained by the CMS collaboration [3], through a combined analysis of off-shell and on-shell events, where two scenarios are considered: $\Gamma_H = \Gamma_H^{SM} = 4.1$ GeV, or Γ_H left unconstrained. The sign of the relative phase between a_i and a_1 is absorbed into the definition of f_{ai} . [53].

Parameter in units $\times 10^{-5}$	Scenario	Observed at 95% CL
f_{a2}	$\Gamma_H = \Gamma_H^{SM}$	[- 32,514]
	Γ_H unconstrained	[- 38,503]
f_{a3}	$\Gamma_H = \Gamma_H^{SM}$	[- 46,107]
	Γ_H unconstrained	[- 46,110]
f_{Λ_1}	$\Gamma_H = \Gamma_H^{SM}$	[- 11,46]
	Γ_H unconstrained	[- 10,47]

The coupling fractions are also useful to study the limits on the anomalous couplings. They can be obtained from the cross sections ratios of Eq. (26) as

$$\frac{a_i^{ZZ}}{a_j^{ZZ}} = \sqrt{\frac{|f_{ai}^{ZZ}| \alpha_{jj}^{2e2\mu}}{|f_{aj}^{ZZ}| \alpha_{ii}^{2e2\mu}}} \text{sign}(f_{ai}^{ZZ} f_{aj}^{ZZ}). \quad (27)$$

B. The standard model effective field theory framework

A recent approach well-suited for the analysis of anomalous couplings is offered by the standard model effective field theory (SMEFT). The effective Lagrangian up to dimension six includes 2499 effective operators \mathcal{O}_i [55]

$$\mathcal{L}_{\text{SMEFT}} = \mathcal{L}_{\text{SM}} + \sum_i^{2499} C_i \mathcal{O}_i, \quad (28)$$

where the Wilson coefficients C_i along with the SM parameters constitute the parameter space of the SMEFT, whereas the operators \mathcal{O}_i can be described via the Warsaw basis [56], the SILH basis [57] or the Higgs boson basis [58]. These bases are equivalent and their Wilson coefficients can be mapped onto each other. The Higgs basis is well suited to study the Higgs boson interactions at the LHC, though this is not always true: for instance, the parameter space of diboson production at the LHC is larger in the Higgs boson basis than in other ones. In the Higgs boson basis [12], the lowest dimension effective Lagrangian for the HZZ interaction can be written, after a redefinition of the

couplings, as follows

$$\mathcal{L} = \frac{H}{v} \left[(1 + \delta c_z) \frac{(g_L^2 + g_Y^2) v^2}{4} Z_\mu Z^\mu + c_{zz} \frac{g_L^2 + g_Y^2}{4} Z_{\mu\nu} Z^{\mu\nu} + c_{z\Box} g_L^2 Z_\mu \partial_\nu Z^{\mu\nu} + \tilde{c}_{zz} \frac{g_L^2 + g_Y^2}{4} Z_{\mu\nu} \tilde{Z}^{\mu\nu} \right], \quad (29)$$

where v is the vacuum expectation value (VEV) of the Higgs field and g_L, g_Y stand for the $SU(2)_L \times U_Y(1)$ coupling constants, which in a more usual notation read $g_L = g$ and $g_Y = g'$. In this Lagrangian the Higgs boson couplings $\delta c_z, c_{zz}, c_{z\Box}$, and \tilde{c}_{zz} are assumed to be real [12]. The Lagrangian (29) can be straightforwardly written in a more familiar form

$$\mathcal{L} = \frac{g}{2c_W m_Z} H \left[(1 + \delta c_z) m_Z^2 Z_\mu Z^\mu + c_{zz} \frac{g_L^2 + g_Y^2}{4} Z_{\mu\nu} Z^{\mu\nu} + c_{z\Box} g_L^2 Z_\mu \partial_\nu Z^{\mu\nu} + \tilde{c}_{zz} \frac{g_L^2 + g_Y^2}{4} Z_{\mu\nu} \tilde{Z}^{\mu\nu} \right], \quad (30)$$

which allows one to identify the following relations with the form factors of Lagrangian (7)

$$\delta c_z = a_Z \quad (31)$$

$$c_{zz} = \frac{4}{g_L^2 + g_Y^2} \hat{b}_Z, \quad (32)$$

$$c_{z\Box} = \frac{1}{g_L^2} \hat{c}_Z, \quad (33)$$

$$\tilde{c}_{zz} = \frac{4}{g_L^2 + g_Y^2} \tilde{b}_Z, \quad (34)$$

they agree with those relations reported in Ref. [53].

III. ANALYTICAL RESULTS

We now turn to present our analytical results for the one-loop contributions to the HZZ coupling. Since we are considering that either one Z gauge boson or the Higgs boson H are off-shell, we need to address the problem of the gauge dependence of off-shell Green's functions. To deal with this issue and obtain well-behaved vertex functions, there are two well-known approaches: the first one is the so-called pinch technique (PT) [59], which is a diagrammatic approach that allows one to systematically obtain gauge-independent and well-behaved off-shell Green's functions by combining contributing self-energy, vertex, and box diagrams to a physical process, but because of the huge number of necessary Feynman diagrams it may turn into a very cumbersome task. Nevertheless, it was shown that the results obtained up to one-loop level via the PT are equivalent to those obtained via the background field method (BGM) in the Feynman-t'Hooft gauge [60, 61]. In this work, we use the latter method to obtain gauge independent form factors for the HZZ coupling as the number of contributing Feynman diagrams is less than in the PT approach.

For the analytical calculation, we used the Mathematica package FeynArts [62], which allows one to obtain the complete set of Feynman diagrams and their corresponding invariant amplitudes via the background field method. We then used FeynHelpers and FeynCalc [63–65] to perform the tensor decomposition and obtain results in terms of Passarino-Veltman scalar functions, which can be numerically evaluated via either the LoopTools [66] or the Collier [67] packages. The Feynman diagrams that contribute at the one-loop level to the HZZ vertex can be classified into three types according to the particles circulating into the loop: in Fig 2 we show those Feynman diagrams arising from the fermion contribution, whereas in Figs. 3 and 4 we show the Feynman diagrams for the W contribution and the $H - Z$ contribution, respectively. For simplicity, each one of those contributions will be denoted by the subscripts \mathcal{F} , \mathcal{W} , and \mathcal{HZ} , respectively.

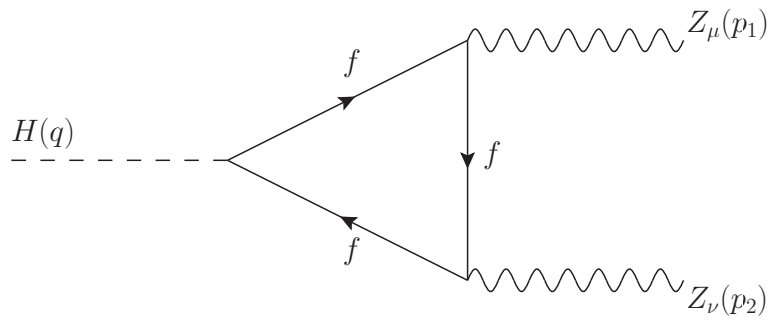


FIG. 2. Feynman diagram for the fermion contribution to the HZZ coupling at the one-loop level.

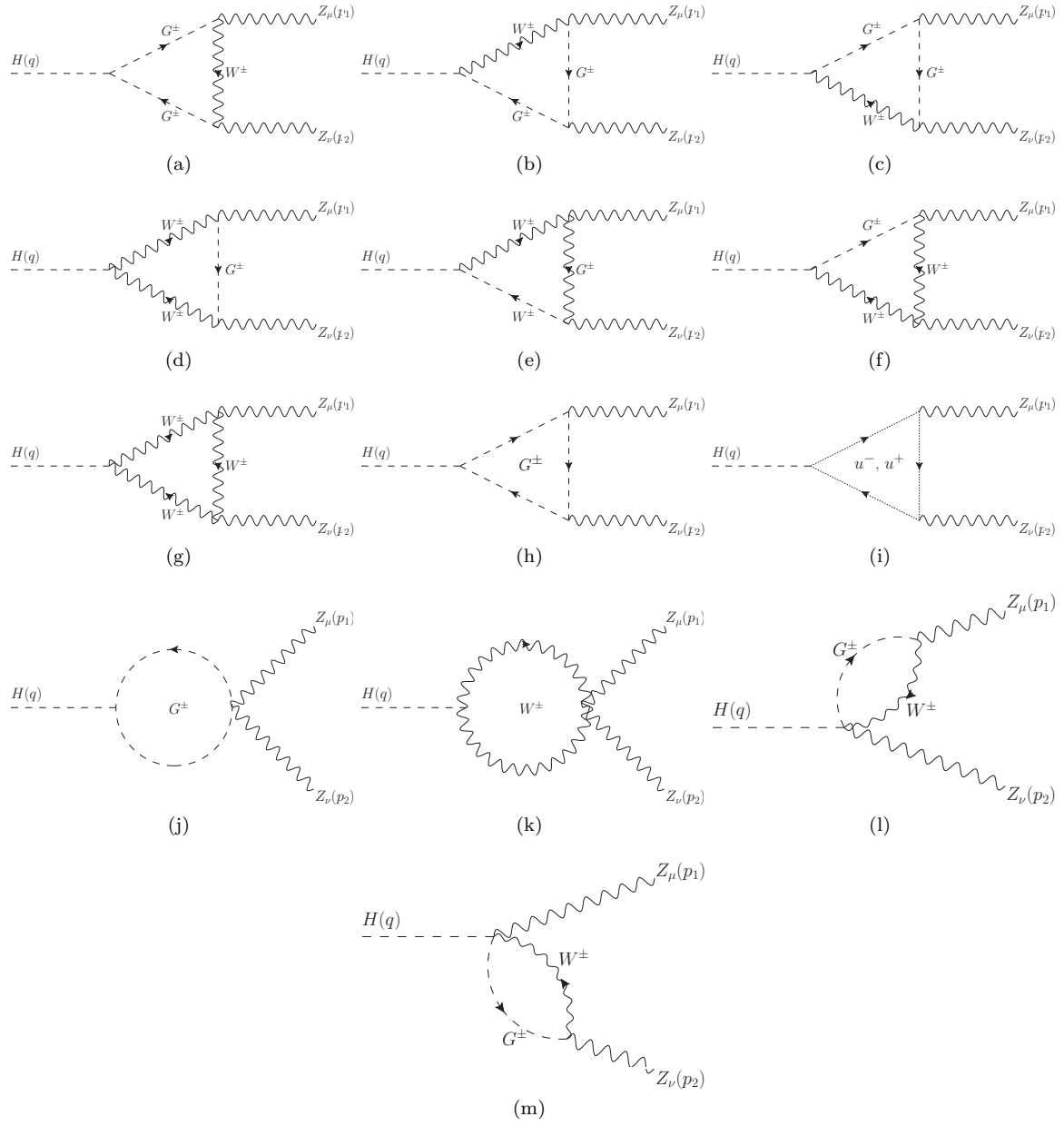


FIG. 3. The same as in Fig. 2 but for the contribution of W gauge boson exchange.

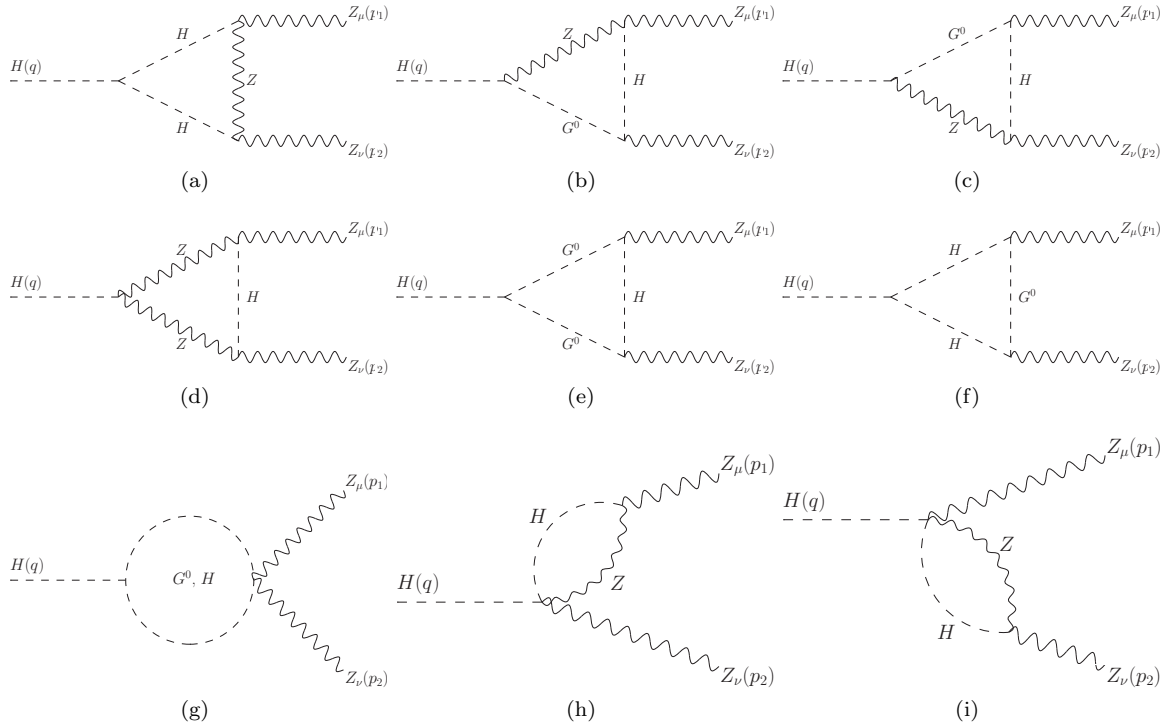


FIG. 4. The same as in Fig. 2 but for the contribution of $H - Z$ boson exchange.

Since obtaining the SM contributions to the anomalous couplings are the main aim of this work, we will focus on the h_2^V form factor, and in the rest of this work $a_Z = 0$. Therefore, following the notation of Ref. [45] our results can be written as

$$h_2^V(q^2, p_1^2, m_Z^2) = m_Z \frac{g^2}{4\pi^2 c_W m_W} \left[\sum_f N_f m_f^2 \{ g_{Vf}^2 A_{Vf}^V(q^2, p_1^2, m_Z^2) + g_{Af}^2 A_{Af}^V(q^2, p_1^2, m_Z^2) \} \right. \\ \left. + A_W^V(q^2, p_1^2, m_Z^2) + A_{ZH}^V(q^2, p_1^2, m_Z^2) \right], \quad (35)$$

where $g_{Vf, Af}$ are the Z boson couplings to fermion pairs:

$$g_{Vf} = \frac{I_f}{2} - Q_f s_W^2, \quad g_{Af} = \frac{I_f}{2}, \quad (36)$$

with I_f and Q_f the fermion weak isospin and electric charge.

The analytic expressions for the $A_{Vf, Af}^V$, A_W^V and A_{ZH}^V functions in terms of Passarino-Veltman scalar functions are too lengthy and are presented in Appendix A. We present explicit results for the contributions to the H^*ZZ ($p_1^2 = m_Z^2$) and HZZ^* ($q^2 = m_H^2$) couplings. We note that for the H^*ZZ coupling, our results agree with those reported in Ref. [45], though there seems to be a difference of sign in the factors of all three-point scalar function C_0 , which stems from the fact that there is an additional minus sign in the definition of such functions in [45] as compared to the usual definition presented in Appendix A. We would like to emphasize that, to our knowledge, the results for the HZZ^* ($q^2 = m_H^2$) coupling have never been reported in the literature. Thus, we present a more comprehensive calculation, which could allow us to assess the anomalous contributions to HZZ coupling in distinct scenarios. The Mathematica code for our analytical results is available for the interested reader [68]. We also include master formulas for the general case where the three particles are off-shell, which are too cumbersome to be presented in this work. Our expressions reported in Appendix A can be straightforwardly obtained from such master formulas.

It is interesting to note that the HZZ form factors are gauge-dependent, as expected, except for the fermion contribution, which evidently does not depend on the gauge-fixing parameter. On the other hand, the three contributions are free of ultraviolet divergences.

IV. NUMERICAL ANALYSIS

We now turn to present the numerical analysis. For the evaluation of the Passarino-Veltman scalar functions, we used the LoopTools package [66] and a cross-check was done via the Collier routines [67]. A good agreement was found between both numerical evaluations. The H^*ZZ and HZZ^* form factors are studied in an energy interval that allows on-shell final bosons.

A. H^*ZZ form factor

We show in Figs. 5(a) and 5(b) the real and imaginary parts of the fermion (\mathcal{F}), W gauge boson (\mathcal{W}), and $H-Z$ boson (\mathcal{HZ}) contributions, along with the total contributions to the H^*ZZ form factor as functions of the Higgs boson transfer momentum $\|q\|$. As for the real part of h_2^H , it is dominated by the \mathcal{W} contribution, whereas \mathcal{F} and \mathcal{HZ} are only relevant at low energies, in such a region they have a similar magnitude to \mathcal{W} . From $\|q\| = 300$ GeV onwards, the \mathcal{F} and \mathcal{HZ} contributions are of similar size but of opposite sign and therefore tend to cancel each other out. It is also interesting to note that the fermion contribution is mainly dominated by the top quark, whereas all other fermions yield negligible contributions. As far as the imaginary part of the h_2^H form factor is concerned, we observe that the \mathcal{W} contribution is also the dominant one, whereas \mathcal{F} and \mathcal{HZ} are one order of magnitude below. As expected, the absorptive part of the \mathcal{F} contribution is non-vanishing only above the threshold $\|q\| = 2m_t$, where the two top quarks attached to the off-shell Higgs boson can be on-shell. In general, the real and imaginary parts of h_2^H are of similar size, as large as $10^{-2} - 10^{-3}$, nevertheless, at high energies, the absorptive part can reach larger values than the real part. This behavior was also observed in other off-shell form factors, see for instance [38–42].

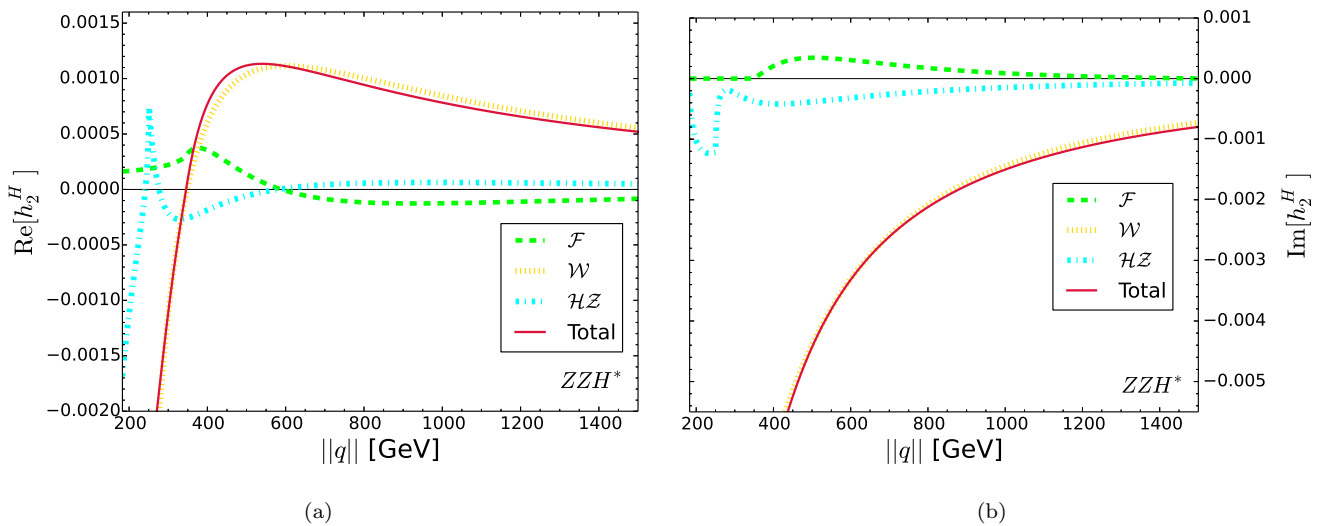


FIG. 5. One loop contributions to the real (left plot) and absorptive (right plot) parts of the form factor h_2^H as functions of the Higgs boson transfer momentum $\|q\|$: fermion (\mathcal{F}), W gauge boson (\mathcal{W}), $H-Z$ bosons (\mathcal{HZ}) and total contributions.

For illustration purposes, the values of the real and imaginary parts of the h_2^H form factors at a few $\|q\|$ values are presented in Table III, along with the values for \hat{b}_Z , a_2^{ZZ} and c_{zz} , which can be obtained from Eqs. (9), (15) and (32), respectively. In effective field theories, the couplings are taken as constant and do not depend on $\|q\|$, but our results can be useful to constrain the energy scale Λ of the model.

TABLE III. Total contributions to the h_2^H form factor for a few values of $\|q\|$. The respective values of \hat{b}_Z , a_2^{ZZ} and c_{zz} are also shown. All these results are in units of 10^{-3} .

$\ q\ $	h_2^H	\hat{b}_Z	a_2^{ZZ}	c_{zz}
190	$-12.99 - 14.02 i$	$-6.49 - 7.01 i$	$12.99 + 14.02 i$	$-48.16 - 51.98 i$
220	$-6.82 - 13.86 i$	$-3.42 - 6.93 i$	$6.82 + 13.86 i$	$-25.3 - 51.4 i$
350	$0.09 - 7.77 i$	$0.04 - 3.88 i$	$-0.09 + 7.77 i$	$0.35 - 28.8 i$
450	$1.02 - 5.24 i$	$0.51 - 2.62 i$	$-1.02 + 5.24 i$	$3.81 - 19.43 i$
600	$1.11 - 3.31 i$	$0.55 - 1.65 i$	$-1.11 + 3.31 i$	$4.12 - 12.29 i$
1000	$0.78 - 1.5 i$	$0.39 - 0.75 i$	$-0.78 + 1.5 i$	$2.9 - 5.56 i$
1500	$0.52 - 0.79 i$	$0.26 - 0.39 i$	$-0.52 + 0.79 i$	$1.92 - 2.95 i$

B. HZZ^* form factor

We now show in Fig. 6 the behavior of the real and imaginary parts of the partial and total contributions to the HZZ^* form factor as functions of the off-shell Z gauge boson transfer momentum $\|p_1\|$. We observe that the h_2^Z form factor has a similar behavior to that of h_2^H . In both cases the \mathcal{W} contribution dominates, but at low energies, the \mathcal{F} and \mathcal{HZ} contributions may be of similar magnitude to \mathcal{W} , whereas at high energies they are negligible. However, there is a slight difference with the behavior of h_2^H , since for both the real and imaginary parts we obtain different values for the h_2^Z case.

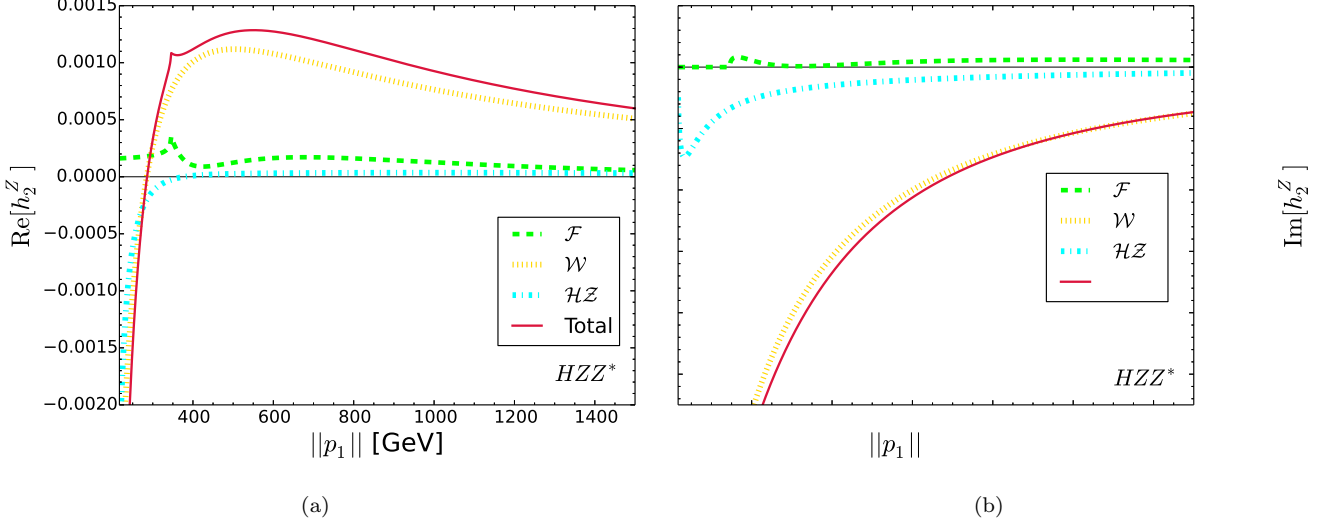


FIG. 6. The same as in Fig. 5, but for the form factor h_2^Z as a function of off-shell Z gauge boson transfer momentum $\|p_1\|$.

In Table IV, we present numerical values for the real and absorptive parts of h_2^Z at a few values of $\|p_1\|$. We also present the respective values for \hat{b}_Z , a_2^{ZZ} and c_{zz} . We can observe that at some energy values, the h_2^Z form factor is larger than the h_2^H one, reaching values of the order of $10^{-2} - 10^{-3}$. It is also noted that for both H^*ZZ and HZZ^* cases, the real and absorptive parts of the anomalous coupling \hat{b}_Z are of the order of $10^{-3} - 10^{-4}$, which agrees with [28]. On the experimental side, the current bounds on \hat{b}_Z are of the same order of magnitude, and thus this anomalous coupling may be measured at the LHC in a near future.

TABLE IV. The same as in Table III, but for the form factor h_2^Z for as a function of $\|p_1\|$.

$\ p_1\ $	h_2^Z	\hat{b}_Z	a_2^{ZZ}	c_{zz}
220	$-4.84 - 15.16 i$	$2.42 + 7.58 i$	$4.84 + 15.16 i$	$17.93 + 56.19 i$
350	$1.07 - 7.37 i$	$-0.53 + 3.68 i$	$-1.07 + 7.37 i$	$-3.98 + 27.33 i$
450	$1.21 - 5.11 i$	$-0.6 + 2.55 i$	$-1.21 + 5.11 i$	$-4.49 + 18.95 i$
600	$1.27 - 3.35 i$	$-0.63 + 1.67 i$	$-1.27 + 3.35 i$	$-4.72 + 12.41 i$
1000	$0.92 - 1.46 i$	$-0.46 + 0.73 i$	$-0.92 + 1.46 i$	$-3.43 + 5.43 i$
1500	$0.59 - 0.73 i$	$-0.29 + 0.36 i$	$-0.59 + 0.73 i$	$-2.22 + 2.71 i$

V. BOUNDS ON THE ANOMALOUS COUPLINGS

Up here nothing has been said about the \hat{c}_Z and \tilde{b}_Z anomalous couplings. Limits on their real and absorptive parts have been set in the past [28], nonetheless, the energy dependence has not been considered. Also, the current CMS bounds [3] only consider constraints on the ratios of such couplings, which cannot be used to assess the corresponding contributions to physical observables [28]. Furthermore, they will play a relevant role as the recent measurement of the $H^* \rightarrow ZZ$ process, and therefore individual constraints on each one of the anomalous couplings are necessary. With this aim, we proceed as follows. Firstly, using Eq. (27) and the values of Table I we use the constraints from Table II to obtain limits on the ratios a_i^{ZZ}/a_2^{ZZ} , which are presented in Table V, where we only consider the scenario with $\Gamma_H = \Gamma_H^{SM}$ as the bounds in the unconstrained scenario yield limits of similar size. Since the CMS constraints are in terms of the LHC framework we use such notation in the rest of this section but the results are also translated to the other contexts considered in this work.

TABLE V. Allowed intervals at 95 % CL for the ratios defined in Eq. (27), where we consider the case $\Gamma_H = \Gamma_H^{SM}$ and the limits of Table II.

Ratio	Allowed values
a_3^{ZZ}/a_2^{ZZ}	$[-1.84, 0.70]$
κ_1^{ZZ}/a_2^{ZZ}	$[-0.35, 0.18]$

Secondly, we use the constraints on a_i^{ZZ}/a_2^{ZZ} of Table V, Eqs. (9), (24) and (25), along with the numerical results from Sec. IV, to find the allowed areas of the real parts of a_3^{ZZ} and κ_1^{ZZ} as functions of the Higgs boson transfer momentum. Also, since the results of Table III indicate that the real and absorptive parts of the H^*ZZ form factor are of similar size, we assume that the limits of Table V are also valid for the imaginary parts of a_3^{ZZ} and κ_1^{ZZ} , which allows us to set constraints on $\text{Im}[a_3^{ZZ}]$ and $\text{Im}[\kappa_1^{ZZ}]$. For our calculations, we use the numerical values of the form factor h_2^H , but the same results are expected for h_2^Z . Moreover, only energy regions where both Z gauge bosons can be on-shell are considered in our analysis.

We thus show in Figs. 7(a) and 7(b) the allowed areas on the planes $\|q\|$ vs $\text{Re}[a_3^{ZZ}]$ and $\|q\|$ vs $\text{Im}[a_3^{ZZ}]$. It is observed that for small values of $\|q\|$ the allowed values for $\text{Re}[a_3^{ZZ}]$ are in the $[-10^{-2}, 10^{-2}]$ interval, nevertheless, this interval shrinks considerably as the energy increases, and at high energies, $\text{Re}[a_3^{ZZ}]$ is only allowed to have values around 10^{-4} . It is also worth noting that around $\|q\| = 320$ GeV, the permitted area for $\text{Re}[a_3^{ZZ}]$ reduces considerably, which stems from the fact that in such a region the real part of a_2^{ZZ} changes sign and $\text{Re}[a_2^{ZZ}] \approx 0$ (see Fig. 5(a)). Therefore, very small values of $\text{Re}[a_3^{ZZ}]$ are required to get a_3^{ZZ}/a_2^{ZZ} inside the allowed region. As for $\text{Im}[a_3^{ZZ}]$, we observe that for small energies the allowed area is large but becomes smaller as the energy increases with the permitted values being of order $10^{-2} - 10^{-3}$. In this case, there is no abrupt shrinkage of the allowed area as in the case of the real part: it turns out that the absorptive part of a_2^{ZZ} does not flip sign in the considered energy range.

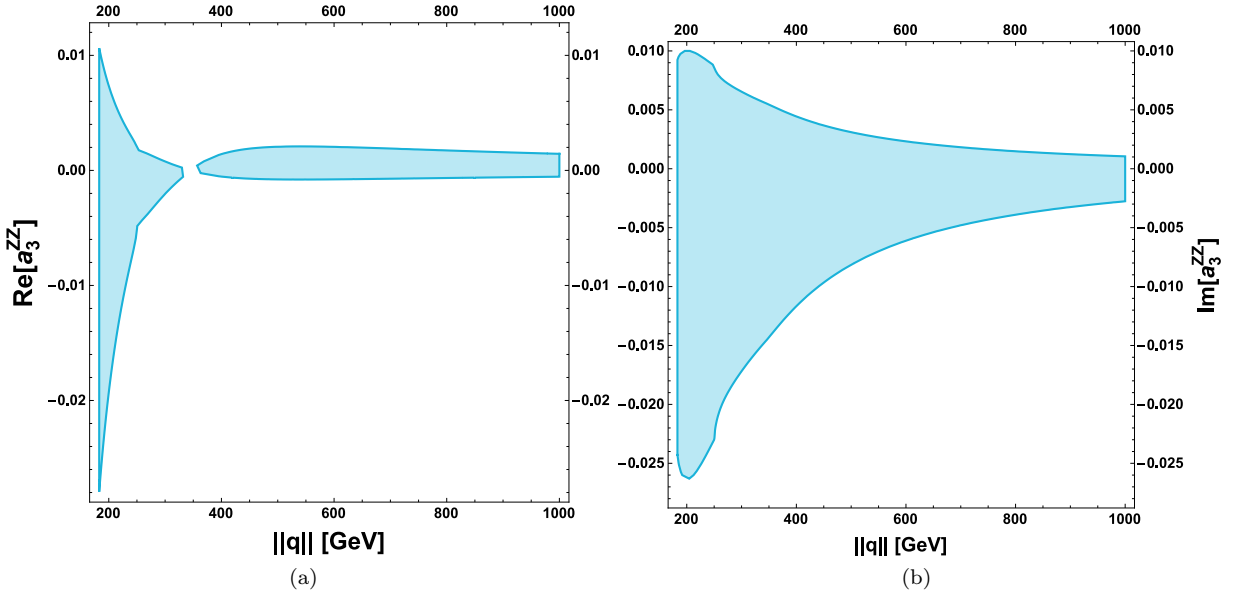


FIG. 7. Allowed area at 95% CL for the the real (left plot) and absorptive (right plot) parts of a_3^{ZZ} as functions of $\|q\|$. These results are compatible with the bounds of Table V.

We now show the allowed areas of the real and absorptive parts of κ_1^{ZZ} as functions of $\|q\|$ in Figs. 8(a) and 8(b), respectively. The results are similar to those obtained for a_3^{ZZ} . Nevertheless, in this case, the allowed upper values of both the real and imaginary parts of a_3^{ZZ} are of the order of 10^{-3} at low energies and become smaller as the energy increases. It is noted that in general, the constraints on the CP violating form factor a_3^{ZZ} are less tighter than those on the CP conserving one κ_1^{ZZ} , although both can be of the same order of magnitude in some energy regions.

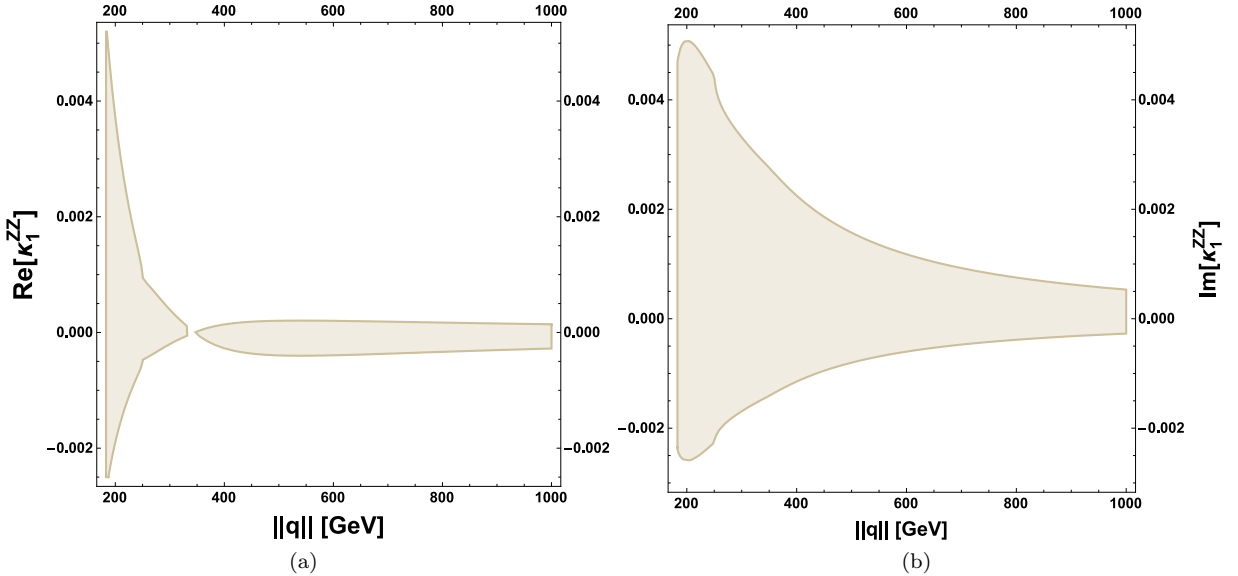


FIG. 8. The same as in Fig. 7, but for the κ_1^{ZZ} form factor.

Our constraints on the form factors a_3^{ZZ} and κ_1^{ZZ} , which correspond to the LHC parametrization, can be translated into constraints on the form factors used in other parametrizations via the relations of Sec. II. In this way we can straightforwardly obtain the allowed regions for \hat{b}_Z , \hat{c}_Z , \tilde{c}_{zz} and $c_{z\Box}$, which are used by other authors in their analysis of the HZZ coupling. For instance, in the SMEFT the anomalous couplings do not depend on the off-shell boson

transfer momenta [69] but the energy parameter Λ , which is related to the scale where the effective model remains valid, has been absorbed in the definition of the Wilson coefficients \tilde{c}_{zz} and $c_{z\Box}$. Hence, our result may be used to set a bound on the energy scale Λ . The corresponding limits are presented in Tables VI and VII. We find that the real and imaginary parts of the CP violating form factors \tilde{b}_Z and \tilde{c}_{zz} are in general of order 10^{-4} , whereas in the SMEFT they can be as large as 10^{-2} for some values of $\|q\|$. The current bounds on the real and absorptive parts of \tilde{b}_Z are of the order of 10^{-3} [28], therefore it is noted that our limits are more stringent. On the other hand, the CP conserving form factor \hat{c}_Z can be as large as 10^{-3} at low energies, which is one order of magnitude smaller than previous results [18]. In the SMEFT, $c_{z\Box}$ can be in general of the order of $10^{-3} - 10^{-4}$ and decreases at high energies.

TABLE VI. Allowed intervals of the real and absorptive parts of the CP violating form factor of the HZZ coupling for a few values of the transfer momentum. We consider three different schemes: the LHC framework (a_3^{ZZ}), a general effective Lagrangian approach (\tilde{b}_Z) and the SMEFT (\tilde{c}_{zz}).

$\ q\ $	$\text{Re}[a_3^{ZZ}]$	$\text{Re}[\tilde{b}_Z]$	$\text{Re}[\tilde{c}_{zz}]$	$\text{Im}[a_3^{ZZ}]$	$\text{Im}[\tilde{b}_Z]$	$\text{Im}[\tilde{c}_{zz}]$
190	$[-0.024, 0.009]$	$[-0.0045, 0.012]$	$[-0.033, 0.088]$	$[-0.026, 0.01]$	$[-0.005, 0.013]$	$[-0.037, 0.096]$
285	$[-0.0029, 0.0011]$	$[-0.00055, 0.0014]$	$[-0.004, 0.01]$	$[-0.018, 0.0069]$	$[-0.0034, 0.009]$	$[-0.025, 0.066]$
400	$[-0.00053, 0.0014]$	$[-0.0007, 0.00026]$	$[-0.0051, 0.0019]$	$[-0.012, 0.0044]$	$[-0.0022, 0.006]$	$[-0.016, 0.044]$
800	$[-0.00069, 0.0018]$	$[-0.0009, 0.00034]$	$[-0.0066, 0.0025]$	$[-0.0039, 0.0015]$	$[-0.00075, 0.0019]$	$[-0.0055, 0.014]$
1500	$[-0.00036, 0.00095]$	$[-0.00047, 0.00018]$	$[-0.0034, 0.0013]$	$[-0.0015, 0.00057]$	$[-0.00028, 0.00075]$	$[-0.002, 0.0055]$

TABLE VII. Allowed intervals for the real and absorptive parts of one of the CP conserving form factors of the HZZ coupling for a few values of the transfer momentum. We consider three different schemes: the LHC framework (κ_1^{ZZ}), a general effective Lagrangian approach (\hat{c}_Z) and the SMEFT ($\tilde{c}_{z\Box}$). From Eq. (25) we note that $\kappa_1^{ZZ} = \hat{c}_Z$.

$\ q\ $	$\text{Re}[\kappa_1^{ZZ}]$ ($\text{Re}[\hat{c}_Z]$)	$\text{Re}[c_{z\Box}]$	$\text{Im}[\kappa_1^{ZZ}]$ ($\text{Im}[\hat{c}_Z]$)	$\text{Im}[c_{z\Box}]$
190	$[-0.0024, 0.0046]$	$[-0.0058, 0.011]$	$[-0.0026, 0.005]$	$[-0.0063, 0.012]$
285	$[-0.00028, 0.00055]$	$[-0.00068, 0.0013]$	$[-0.0018, 0.0035]$	$[-0.0043, 0.0085]$
400	$[-0.00027, 0.00014]$	$[-0.00065, 0.00034]$	$[-0.0012, 0.0023]$	$[-0.0029, 0.0055]$
800	$[-0.00034, 0.00017]$	$[-0.00082, 0.00041]$	$[-0.00038, 0.00075]$	$[-0.00092, 0.0018]$
1500	$[-0.00019, 0.0001]$	$[-0.00046, 0.00024]$	$[-0.00015, 0.00029]$	$[-0.00036, 0.0007]$

VI. THE $H^* \rightarrow ZZ$ PROCESS

In this section, we study the effects of the anomalous couplings on the partial decay width of the $H^* \rightarrow ZZ$ process. The virtuality of the Higgs boson in physical observables as the cross-sections and partial widths have been defined in Ref. [70]. Nonetheless, the imaginary parts of the HZZ coupling and their implications on such observables have not been discussed in the literature. To study their role in the Z boson pair production, we consider the anomalous couplings of the HZZ vertex as complex quantities and express the h_i^H form factors as

$$h_i^H = \text{Re}[h_i^H] + i\text{Im}[h_i^H]. \quad (37)$$

In terms of the h_i^H form factors, the invariant amplitude for the production of two on-shell Z gauge bosons from an off-shell Higgs boson can be written in the following form

$$\begin{aligned} \mathcal{M}(\lambda_1, \lambda_2) = & \frac{g}{c_W} m_Z \left\{ g^{\mu\nu} \left(\text{Re}[h_1^H] + i\text{Im}[h_1^H] \right) + \frac{p_2^\mu p_1^\nu}{m_Z^2} \left(\text{Re}[h_2^H] + i\text{Im}[h_2^H] \right) \right. \\ & \left. + \frac{\epsilon^{\mu\nu\alpha\beta} p_{1\alpha} p_{2\beta}}{m_Z^2} \left(\text{Re}[h_3^H] + i\text{Im}[h_3^H] \right) \right\} \epsilon_\mu^*(p_1, \lambda_1) \epsilon_\nu^*(p_2, \lambda_2), \end{aligned} \quad (38)$$

where λ_i stands for the polarizations of the $Z(p_i)$ gauge bosons and $\epsilon_\mu(p_1)$ and $\epsilon_\nu(p_2)$ are their corresponding polarization vectors. We would like to stress that that the terms $\text{Im}[h_1^H]$, $\text{Im}[h_2^H]$ and $\text{Im}[h_3^H]$ have not been considered in previous studies of the $H^* \rightarrow ZZ$ process [34, 45].

A. The unpolarized case

From the amplitude (38), the partial decay width in terms of the real and adsorptive parts of the h_i^H form factors can be obtained:

$$\begin{aligned} \Gamma_{H^* \rightarrow ZZ} = & \frac{g^2 \sqrt{q^2 - 4m_Z^2}}{512\pi q^2 c_W^2 m_Z^6} \left\{ 4q^6 m_Z^2 \left((\text{Im}[h_1^H] - 2\text{Im}[h_2^H]) \text{Im}[h_2^H] + (\text{Re}[h_1^H] - 2\text{Re}[h_2^H]) \text{Re}[h_2^H] \right) \right. \\ & + 4q^4 m_Z^4 \left(2 \left(2\text{Im}[h_2^H]^2 + \text{Im}[h_3^H]^2 + 2\text{Re}[h_2^H]^2 + \text{Re}[h_3^H]^2 \right) + \text{Im}[h_1^H]^2 - 6\text{Im}[h_2^H] \text{Im}[h_1^H] \right. \\ & + \left. \left. \text{Re}[h_1^H]^2 - 6\text{Re}[h_1^H] \text{Re}[h_2^H] \right) - 16q^2 m_Z^6 \left(2 \left(\text{Im}[h_3^H]^2 + \text{Re}[h_3^H]^2 \right) + \text{Im}[h_1^H]^2 - 2\text{Im}[h_2^H] \text{Im}[h_1^H] \right. \right. \\ & \left. \left. + \text{Re}[h_1^H]^2 - 2\text{Re}[h_1^H] \text{Re}[h_2^H] \right) + 48m_Z^8 \left(\text{Im}[h_1^H]^2 + \text{Re}[h_1^H]^2 \right) + q^8 \left(\text{Im}[h_2^H]^2 + \text{Re}[h_2^H]^2 \right) \right\}, \end{aligned} \quad (39)$$

which reduces to the SM tree-level result [45] when $\text{Re}[h_1^H] = 1$, $\text{Re}[h_{2,3}^H] = \text{Im}[h_{1,2,3}^H] = 0$:

$$\Gamma_{H^* \rightarrow ZZ}^{\text{Tree}} = \frac{g^2 \sqrt{q^2 - 4m_Z^2}}{512\pi c_W^2 m_Z^6} \left(4q^2 m_Z^4 - 16m_Z^6 + 48 \frac{m_Z^8}{q^2} \right). \quad (40)$$

The tree and one-loop SM contributions to the $H^* \rightarrow ZZ$ decay have been studied long ago [34, 45]. Nevertheless, the entire set of anomalous couplings has not been considered yet and their implications remain unexplored. Thus, a complete analysis is required since the HZZ non-SM couplings may be at the reach of measurement soon. To examine their effects on Z gauge bosons pair production from an off-shell Higgs boson, we define the ratio \mathcal{R} between the general and the SM tree level partial widths

$$\mathcal{R} = \frac{\Gamma_{H^* \rightarrow ZZ}}{\Gamma_{H^* \rightarrow ZZ}^{\text{Tree}}}. \quad (41)$$

Then, to evaluate Eq. (41) we use Eqs. (8), (9), (10) for the h_i^H form factors, which were obtained in terms of the anomalous couplings \hat{b}_Z , \hat{c}_Z and \tilde{b}_Z from Lagrangian (7). The analytical results obtained in Sec. III for \hat{b}_Z are also used for the numerical analysis, whereas for the remaining anomalous couplings, we use values consistent with the bounds of Tables VI, VII. For illustration purposes, in our analysis below, we consider the following scenarios:

- Scenario I: $\text{Re}[\hat{c}_Z] = 0.0001$, $\text{Im}[\hat{c}_Z] = 0.001$, $\text{Re}[\tilde{b}_Z] = 0.0001$ and $\text{Im}[\tilde{b}_Z] = 0.001$.
- Scenario II: $\text{Re}[\hat{c}_Z] = -0.001$, $\text{Im}[\hat{c}_Z] = 0.001$, $\text{Re}[\tilde{b}_Z] = -0.0001$ and $\text{Im}[\tilde{b}_Z] = 0.001$.
- Scenario III: $\text{Re}[\hat{c}_Z] = 0.001$, $\text{Im}[\hat{c}_Z] = -0.0001$, $\text{Re}[\tilde{b}_Z] = 0.0001$ and $\text{Im}[\tilde{b}_Z] = -0.001$.

We show in Fig. 9 the behavior of \mathcal{R} as a function of the Higgs boson transfer momentum $\|q\|$ when only the one-loop SM contribution is considered, namely, $\hat{c}_Z = \tilde{b}_Z = 0$, and also in the three above scenarios. We observe that at high energies \mathcal{R} become constant: the curves for the SM one-loop contribution and that for scenario II approaches the unity, whereas the curves for scenarios I and III show a slight deviation up to around 0.2%. On the other hand, at low energies, the deviation of \mathcal{R} from the unity can be as large as 3% in the four cases, which could allow us to observe the effects of any anomalous couplings to the process $H^* \rightarrow ZZ$. Nevertheless, it may be difficult to discriminate between the SM one-loop contribution and those arising from the \hat{c}_Z and \tilde{b}_Z anomalous couplings.

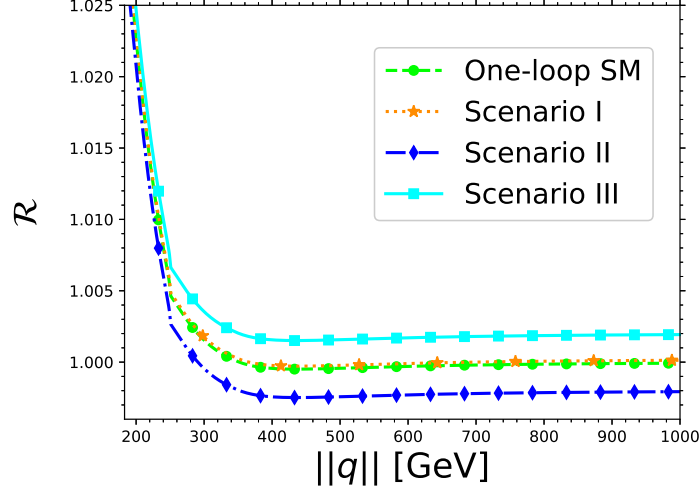


FIG. 9. Behavior of the ratio \mathcal{R} as function of the transfer momentum of the Higgs Boson $\|q\|$ for the one-loop SM contribution, namely, $\hat{c}_Z = \tilde{b}_Z = 0$, and also in the three scenarios discussed in the text for \hat{c}_Z and \tilde{b}_Z . For \tilde{b}_Z we use the expressions obtained in Sec. III.

B. The polarized case

From the amplitude (38) it is also possible to obtain the partial decay width $\Gamma_{H^* \rightarrow ZZ}$ for polarized Z gauge bosons. In the frame in which the vectors bosons propagate along the $x - z$ plane, the polarization vectors can be written as

$$\begin{aligned} \epsilon_{1,2}^\mu(0) &= \frac{1}{m_Z} \left(\|\vec{p}\|, \pm E \sin \theta, 0, \pm E \cos \theta \right), \\ \epsilon_1^\mu(L/R) &= \frac{1}{\sqrt{2}} \left(0, \pm \cos \theta, -i, \mp \sin \theta \right), \end{aligned} \quad (42)$$

where the energy and magnitude of the three momentum can be written as $E = \sqrt{q^2}/2$ and $\|p\| = \sqrt{q^2 - 4m_Z^2}/2$. In terms of the three contributing polarized amplitudes $\mathcal{M}(0, 0)$, $\mathcal{M}(L, L)$, $\mathcal{M}(R, R)$ the squared amplitude is

$$\begin{aligned} \mathcal{M}^2 &= \left(\frac{g}{c_W} \right)^2 m_Z^2 \sum_{\lambda_i} \left(\mathcal{M}^2(\lambda_i, \lambda_i) \right) \\ &= \left(\frac{g}{c_W} \right)^2 m_Z^2 \left(\mathcal{M}_{LL}^2 + \mathcal{M}_{RR}^2 + \mathcal{M}_{00}^2 \right), \end{aligned} \quad (43)$$

with $\mathcal{M}^2(\lambda_i, \lambda_i) \equiv \mathcal{M}_{\lambda_i, \lambda_i}^2$ given by

$$\begin{aligned} \mathcal{M}_{LL}^2 &= \frac{1}{4m_Z^4} \left\{ 4m_Z^2 \sqrt{q^4 - 4q^2 m_Z^2} \left(\text{Re}[h_1^H] \text{Im}[h_3^H] - \text{Im}[h_1^H] \text{Re}[h_3^H] \right) \right. \\ &\quad \left. + q^2 (q^2 - 4m_Z^2) \left(\text{Re}[h_3^H]^2 + \text{Im}[h_3^H]^2 \right) + 4m_Z^4 \left(\text{Re}[h_1^H]^2 + \text{Im}[h_1^H]^2 \right) \right\}, \end{aligned} \quad (44)$$

$$\begin{aligned} \mathcal{M}_{RR}^2 &= \frac{1}{4m_Z^4} \left\{ -4m_Z^2 \sqrt{q^4 - 4q^2 m_Z^2} \left(\text{Re}[h_1^H] \text{Im}[h_3^H] - \text{Im}[h_1^H] \text{Re}[h_3^H] \right) \right. \\ &\quad \left. + q^2 (q^2 - 4m_Z^2) \left(\text{Re}[h_3^H]^2 + \text{Im}[h_3^H]^2 \right) + 4m_Z^4 \left(\text{Re}[h_1^H]^2 + \text{Im}[h_1^H]^2 \right) \right\}, \end{aligned} \quad (45)$$

and

$$\begin{aligned}
\mathcal{M}_{00}^2 = & \frac{1}{16m_Z^8} \left\{ 4q^6 m_Z^2 \left[(\text{Im}[h_1^H] - 2\text{Im}[h_2^H]) \text{Im}[h_2^H] + (\text{Re}[h_1^H] - 2\text{Re}[h_2^H]) \text{Re}[h_2^H] \right] \right. \\
& + 4q^4 m_Z^4 \left[4 (\text{Im}[h_2^H]^2 + \text{Re}[h_2^H]^2) + \text{Im}[h_1^H]^2 - 6\text{Im}[h_2^H] \text{Im}[h_1^H] + \text{Re}[h_1^H]^2 - 6\text{Re}[h_1^H] \text{Re}[h_2^H] \right] \\
& - 16q^2 m_Z^6 \left[\text{Im}[h_1^H]^2 - 2\text{Im}[h_2^H] \text{Im}[h_1^H] + \text{Re}[h_1^H] (\text{Re}[h_1^H] - 2\text{Re}[h_2^H]) \right] \\
& \left. + 16m_Z^8 (\text{Im}[h_1^H]^2 + \text{Re}[h_1^H]^2) + q^8 (\text{Im}[h_2^H]^2 + \text{Re}[h_2^H]^2) \right\}. \tag{46}
\end{aligned}$$

The results for the real case can also be obtained from the amplitudes ¹ of Ref. [7]. Once again, the amplitudes are in terms of the real and absorptive part of the h_i^H form factors, and the polarized partial width can be defined as

$$\Gamma_{H^* \rightarrow Z_{\lambda_i} Z_{\lambda_i}} = \frac{g^2 m_Z^2 \sqrt{q^2 - 4m_Z^2}}{32\pi q^2 c_W^2} \mathcal{M}_{\lambda_i \lambda_i}^2. \tag{47}$$

We note that the CP -violating form factor h_3^H only appears in the \mathcal{M}_{LL}^2 and \mathcal{M}_{RR}^2 amplitudes. Although both polarized square amplitudes seem to be similar, there is a difference of signs in those terms where the real and absorptive parts of h_1^H and h_3^H mix. This peculiarity allows us to introduce an asymmetry, which, to our knowledge, has never been reported in the literature. This left-right asymmetry can be written as

$$\mathcal{A}_{LR} = \frac{\Gamma_{H^* \rightarrow Z_L Z_L} - \Gamma_{H^* \rightarrow Z_R Z_R}}{\Gamma_{H^* \rightarrow Z_L Z_L} + \Gamma_{H^* \rightarrow Z_R Z_R}}, \tag{48}$$

which can be expressed in terms of the real and imaginary parts of the form factors via Eqs. (44) and (45):

$$\mathcal{A}_{LR} = \frac{4m_Z^2 \|q\| \sqrt{q^2 - 4m_Z^2} (\text{Re}[h_1^H] \text{Im}[h_3^H] - \text{Re}[h_3^H] \text{Im}[h_1^H])}{q^2 (q^2 - 4m_Z^2) (\text{Re}[h_3^H]^2 + \text{Im}[h_3^H]^2) + 4m_Z^4 (\text{Im}[h_1^H]^2 + \text{Re}[h_1^H]^2)}. \tag{49}$$

It is worth noting that the size of this asymmetry is dominated by the CP -violating form factor h_3^H as \mathcal{A}_{LR} is proportional to its real and absorptive parts. Therefore, CP violation becomes relevant in the $H^* \rightarrow ZZ$ process when polarized Z gauge bosons are considered. Also, from Eq. (49) we observe that a non-vanishing \mathcal{A}_{LR} is obtained as long as both the absorptive parts of h_1^H and h_3^H are present, which are induced for an off-shell Higgs boson. In summary, the left-right asymmetry is a consequence of two elements: the presence of CP violation and complex form factors. In the past, some asymmetries have been studied through the HZZ couplings [49], though they have a very different origin as are related to the energy of the four-lepton final state. We thus would like to stress the relevance of the imaginary parts of the anomalous couplings in processes where off-shell particles are involved since they have been neglected before, despite they could yield sizeable deviations in several observables.

In the SM, the \mathcal{A}_{LR} asymmetry would vanish up to the two-loop level as the CP -violating form factor h_3^H is supposed to be induced at three-loop level, with a value of the order of 10^{-11} [49]. Therefore, if we consider $\text{Re}[h_3^H] = \text{Im}[h_3^H] \approx 10^{-11}$ and only one-loop SM contributions to the CP conserving form factors, i.e., $\hat{c}_Z = 0$, we obtain the following estimate

$$\mathcal{A}_{LR}^{SM} \approx 10^{-8} - 10^{-9}, \tag{50}$$

for energies up to $\|q\| = 3000$ GeV.

To assess the importance of the CP -violating form factor, together with the complete anomalous couplings contributions and their allowed values obtained in Sec. V, we fix $\text{Re}[\hat{c}_Z] = \text{Im}[\hat{c}_Z] = 0.001$ and consider the following four scenarios:

- Scenario i: $\text{Re}[\tilde{b}_Z] = 0.001$ and $\text{Im}[\tilde{b}_Z] = 0.01$.
- Scenario ii: $\text{Re}[\tilde{b}_Z] = 0.001$ and $\text{Im}[\tilde{b}_Z] = -0.01$.
- Scenario iii: $\text{Re}[\tilde{b}_Z] = 0.0001$ and $\text{Im}[\tilde{b}_Z] = 0.001$.

¹ As we use a different convention for $\epsilon_{1,2}^H(0)$ the amplitude $\mathcal{M}(0,0)$ differs by a minus sign with the result reported in Ref. [7] but the squared amplitude is the same.

- Scenario iv: $\text{Re}[\tilde{b}_Z] = \text{Im}[\tilde{b}_Z] = 0.0001$.

We show in Fig. 10 the behavior of the \mathcal{A}_{LR} asymmetry as a function of the Higgs transfer momentum $\|q\|$ in the four scenarios described above. We first consider scenarios i and ii, where the real and imaginary parts of the CP -violating form factor h_3^H are larger than $\text{Re}[\hat{c}_Z]$ and $\text{Im}[\hat{c}_Z]$. We observe that except for an opposite sign, in both of such scenarios \mathcal{A}_{LR} shows a similar behavior and can reach values close to one, which means that the difference between the production of left-handed and right-handed Z gauge bosons can be as large as the total production of transverse Z gauge bosons. Thus, if we consider the total Z gauge boson production, a lot of information about the properties of Z_L and Z_R is lost as the terms responsible for the asymmetry are canceled. As far as scenarios iii and iv are concerned, \mathcal{A}_{LR} can reach values of the order of 10^{-3} and 10^{-4} , respectively, at low energies, which are still much larger, by about four orders of magnitude, than the SM contribution. In general, we note that in the four scenarios \mathcal{A}_{LR} is small at low energies and reaches its highest values at high energy. This behavior is contrary to that observed for the total Z gauge bosons pair production of Fig. 9, where the anomalous coupling effects can only be observed in the region of low energy. Therefore, the study of polarized Z gauge bosons offers a good opportunity to detect non-SM contributions to the HZZ vertex, since the region where such effects can be discriminated is broader than in the case of the production of unpolarized Z gauge boson pairs. Furthermore, our results may be tested at the LHC as the role of Z_L , Z_R and Z_0 in $H \rightarrow ZZ^* \rightarrow 4\ell$ process has already been explored under the SM and new physics effects [71, 72].

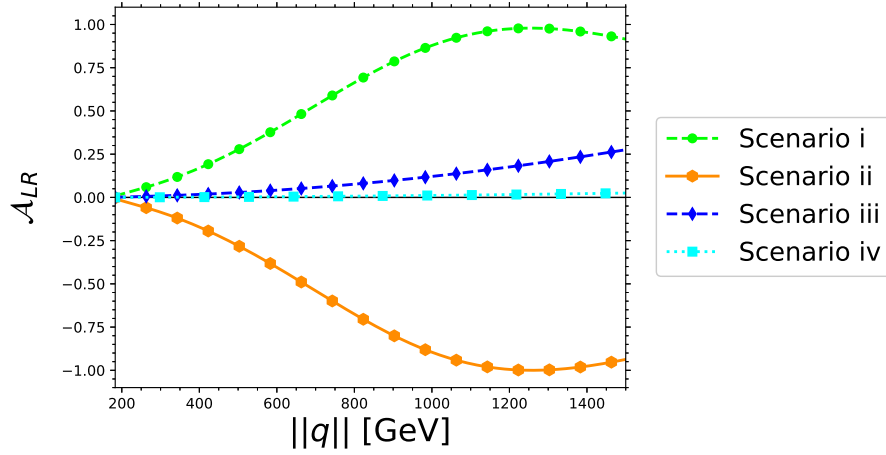


FIG. 10. \mathcal{A}_{LR} asymmetry as a function of the transfer momentum of the Higgs boson $\|q\|$ for the four scenarios described in the text for the real and absorptive parts of the anomalous couplings \hat{c}_Z and \tilde{b}_Z . For \tilde{b}_Z we use the expressions obtained in Sec. III.

For completeness, we show in Fig. 11 the behavior of the partial decay widths $\Gamma_{H^* \rightarrow Z_L Z_L / Z_R Z_R}$ as functions of $\|q\|$ in the same scenarios of Fig. 10, though scenario iv is not considered as it does not yield relevant results. We also include the tree and one-loop level SM results. Again, the anomalous coupling contributions become more marked as the energy increases, which stems from the fact that large deviations from the SM results arising from the CP -violating form factor (scenarios i and ii) are more appreciable at very high energies. This can be explained if we analyze the high energy behavior of Eq. (47), which for transverse polarizations reads

$$\Gamma_{H^* \rightarrow Z_L Z_L / Z_R Z_R} = \frac{g^2 \|q\|}{128\pi c_W^2 m_Z^2} \left\{ \pm 4m_Z^2 \left(\text{Re}[h_1^H] \text{Im}[h_3^H] - \text{Im}[h_1^H] \text{Re}[h_3^H] \right) + q^2 \left(\text{Re}[h_3^H]^2 + \text{Im}[h_3^H]^2 \right) \right\}, \quad (51)$$

where the term related to \mathcal{A}_{LR} in Eq. (49) can be recognized and ensures a non-zero asymmetry at very high energies. In this regime, the main contributions arise from the h_3^H quadratic terms. Thus, as observed in Fig. 11, the CP violating form factor is the main responsible for the deviations from the SM predictions since they are more relevant in the $q^2 \rightarrow \infty$ limit. In summary, the possibility to detect effects of anomalous couplings, and in particular of CP violation, increases for high energy polarized Z gauge bosons. Therefore, the recent measurement of two Z gauge bosons from an off-shell Higgs boson opens up the possibility for the detection of anomalous HZZ couplings in a near future because of the expected LHC upgrades. Moreover, the implications of these new contributions may be observed

in the four lepton final state of the process $H^* \rightarrow ZZ \rightarrow 4\ell$ [72], where any deviation from the SM would be clear evidence of new physics. To our knowledge, only the case $H \rightarrow ZZ^* \rightarrow 4\ell$ has been revisited up to now [7, 49, 50, 71–75], thus we expect that our calculation could be helpful in new studies. Finally, the analysis of the scenario of pair production longitudinally polarized Z gauge bosons is not presented as there is not a relevant difference between the SM and the case where the anomalous couplings contributions are considered.

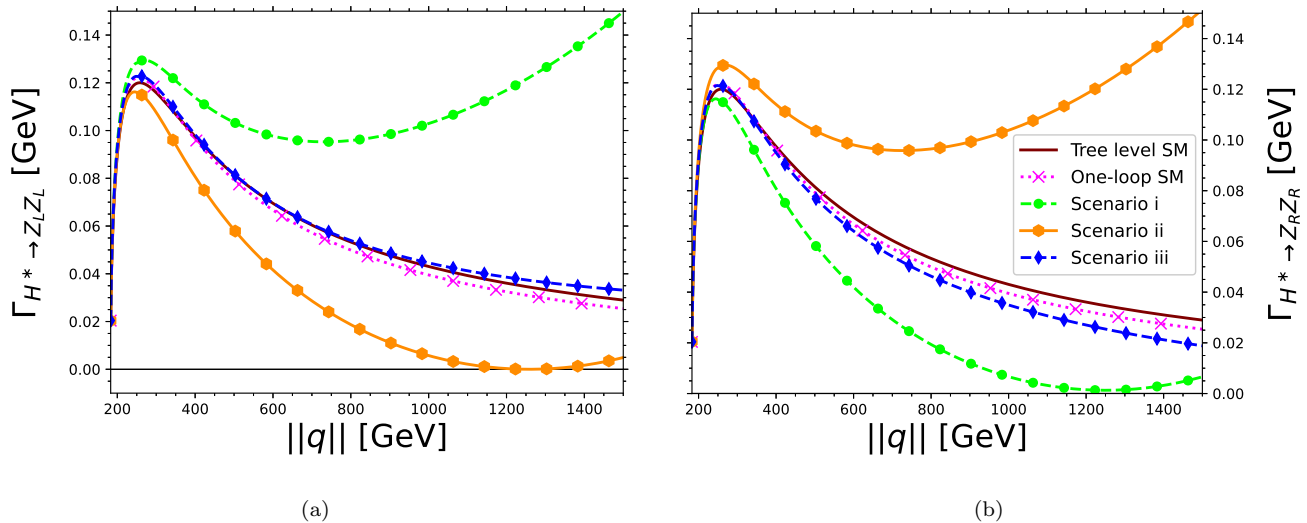


FIG. 11. Partial decay widths of the processes $H^* \rightarrow Z_L Z_L / Z_R Z_R$ as functions of the Higgs boson transfer momentum $\|q\|$ in the first three scenarios of Fig. 10 along with the tree and one-loop level SM predictions.

VII. CONCLUSIONS AND OUTLOOK

Motivated by the recent measurement of Z gauge boson pair production from an off-shell Higgs boson at the LHC, we have presented a calculation of the one-loop SM contributions to the HZZ coupling, which can be written in terms of two CP -conserving $h_{1,2}^V$ and one CP -violating h_3^V form factors, where V stands for the off-shell Higgs boson. Since measurements at future LHC runs could be sensitive to the potential effects of any anomalous contributions to this Higgs boson coupling, an up-to-date calculation is necessary to disentangle any anomalous effects from its SM contributions. We first obtain general results for the contributions to the $H^* Z^* Z^*$ coupling via the background field method in terms of Passarino-Veltman scalar functions, which are too lengthy to be presented here, but are available for the interested reader in an internet repository [68]. From such general results, the corresponding contributions to the $H^* ZZ$ and HZZ^* couplings can be straightforwardly obtained and are reported in Appendix A.

We present an analysis of behavior of the $H^* ZZ$ and HZZ^* couplings, with focus on the effects of their absorptive parts, which have been overlooked in the past. For the numerical analysis, we consider the most popular parametrizations used in the literature, and the relationships necessary to map from one to another parametrization are obtained. In particular, the parametrization used in Lagrangian (7) is the most convenient one as allows one to express the h_2^V form factor in terms of only one anomalous coupling. It is found that the main one-loop SM contributions to the h_2^V ($V = H, Z$) form factor arise from the Feynman diagrams with a virtual W gauge boson. Although h_2^H can be as large as 10^{-2} at low energies, in general, h_2^V can be of the order of $10^{-3} - 10^{-4}$ at high energies. We analyze several scenarios of interest and employing our analytical results along with the current constraints on the HZZ coupling ratios reported by the CMS collaboration, new bounds on the anomalous HZZ couplings are obtained, which are of the order of $10^{-2} - 10^{-4}$ depending on the value of the transfer momentum of the off-shell particle. It is worth emphasizing that while the limits on the real parts of the anomalous HZZ couplings are up to two orders of magnitude tighter than the previous ones, the ones on the absorptive parts are a novel contribution as no previous limits of this kind have been reported before.

To assess the potential effects of the absorptive parts of the HZZ anomalous couplings, we estimate their contributions to the partial decay width $\Gamma_{H^* \rightarrow ZZ}$, which are compared with the SM tree-level contribution. It is found that at low energies the anomalous contributions can yield a deviation on $\Gamma_{H^* \rightarrow ZZ}$ up to 3% from the tree-level SM result,

whereas at high energies there is a negligibly small deviation. Along this line, polarized Z gauge bosons can be useful for the study of non-SM couplings via a new left-right asymmetry \mathcal{A}_{LR} , which is sensitive to CP -violating complex form factors. Such asymmetry can be as large as the unity for large values of the CP -violating form factor, but it is of the order of $10^{-3} - 10^{-4}$ in a more conservative scenario. Such values are indeed still larger by five or four orders of magnitude than the SM prediction for \mathcal{A}_{LR} , which has a non-vanishing contribution up to the three-loop level.

The partial decay widths $\Gamma_{H^* \rightarrow Z_L Z_L}$ and $\Gamma_{H^* \rightarrow Z_R Z_R}$ are also studied in several scenarios of new physics and a comparison is made with the tree and one-loop level SM contributions. Once again, significant deviations from the SM results are due to the CP -violating HZZ form factor. It is observed that such deviations can be large at high energies, and become even larger as the energy increases. Thus, for polarized Z gauge bosons, there is a broad energy interval where the measurements could be sensitive to anomalous contributions, in contrast with the case of unpolarized Z gauge bosons, where there is only sensitivity to anomalous contributions at low energies. Thus, new physics effects may be searched for via the four-lepton final state of the process $H^* \rightarrow ZZ \rightarrow 4\ell$.

ACKNOWLEDGMENTS

We acknowledge support from Consejo Nacional de Ciencia y Tecnología and Sistema Nacional de Investigadores (Mexico). Partial support from Vicerrectoría de Investigación y Estudios de Posgrado de la Benémerita Universidad Autónoma de Puebla is also acknowledged.

Appendix A: Analytical results

In this Appendix we present the analytical expression for the one-loop contributions to the HZZ form factor h_2^V of Eq. (35) in terms of Passarino-Veltman scalar functions, which are obtained from our general results for the form factors of the $H^* Z^* Z^*$ coupling [68].

The two- and three-point Passarino-Veltman scalar functions are defined as

$$B_0(r^2, m_1^2, m_2^2) = \frac{1}{i\pi^2} \int \frac{d^D k}{(k^2 - m_1^2)((k+r)^2 - m_2^2)}, \quad (\text{A1})$$

$$C_0(r_1^2, (r_1 + r_2)^2, r_2^2, m_1^2, m_2^2, m_3^2) = \frac{1}{i\pi^2} \int \frac{d^D k}{(k^2 - m_1^2)((k+r_1)^2 - m_2^2)((k+r_2)^2 - m_3^2)}. \quad (\text{A2})$$

We now introduce the following shorthand notation

$$\begin{aligned} B_{0ij}(r^2) &= B_0(r^2, m_i^2, m_j^2), \\ C_{0ijk}(q^2) &= C_0(m_Z^2, m_Z^2, q^2, m_i^2, m_j^2, m_k^2), \\ C_{0ijk}(p_1^2) &= C_0(m_H^2, m_Z^2, p_1^2, m_i^2, m_j^2, m_k^2), \end{aligned} \quad (\text{A3})$$

It is useful to observe the following symmetry relations

$$\begin{aligned} B_{ij}(r^2) &= B_{ji}(r^2), \\ C_{ijk}(q^2) &= C_{kji}(q^2), \end{aligned} \quad (\text{A4})$$

1. Contributions to the $H^* ZZ$ coupling

The contributions from fermion to the $A_{Vf, Af}^H$ functions read

$$\begin{aligned} A_{Vf}^H(q^2, m_Z^2) &= \frac{1}{q^2 (q^2 - 4m_Z^2)^2} \left\{ 4q^2 m_Z^2 [B_{0ff}(q^2) - B_{0ff}(m_Z^2) - 3] + 8m_Z^4 [B_{0ff}(q^2) - B_{0ff}(m_Z^2) + 2] \right. \\ &\quad \left. - (q^2 - 2m_Z^2) (-4m_f^2 (q^2 - 4m_Z^2) - 6q^2 m_Z^2 - 4m_Z^4 + q^4) C_{0fff}(q^2) + 2q^4 \right\}, \end{aligned} \quad (\text{A5})$$

$$A_{Af}^H(q^2, m_Z^2) = \frac{1}{q^2(q^2 - 4m_Z^2)^2} \left\{ (q^2 - 2m_Z^2) (4(q^2 - m_Z^2) [B_{0ff}(q^2) - B_{0ff}(m_Z^2)] \right. \\ \left. + (-2m_Z^2(8m_f^2 + q^2) + 4q^2m_f^2 + 4m_Z^4 + q^4) C_0(q^2, m_Z^2, m_Z^2, m_f^2, m_f^2, m_f^2) + 2(q^2 - 4m_Z^2) \right\}. \quad (A6)$$

As for the contributions from W gauge boson (W), and $H - Z$ boson (\mathcal{HZ}) exchange, they are given by

$$A_W^H(q^2, m_Z^2) = \frac{1}{8q^2(q^2 - 4m_Z^2)^2} \left\{ 2 \left((1 - 2c_W^2)^2 m_H^2 m_Z^2 (2m_Z^2 + q^2) + 2m_W^2 ((12c_W^4 - 4c_W^2 - 7)q^2 m_Z^2 \right. \right. \\ \left. \left. + (24c_W^4 - 8c_W^2 + 2)m_Z^4 + 2q^4) \right) [B_{0WW}(m_Z^2) - B_{0WW}(q^2)] - 2 \left((1 - 2c_W^2)^2 m_H^2 (2m_Z^4 (q^2 - m_Z^2) \right. \right. \\ \left. \left. + m_W^2 (-6q^2 m_Z^2 + 8m_Z^4 + q^4)) + 2m_W^2 (4c_W^2 (1 - 2c_W^2)q^6 + 2(32c_W^4 - 16c_W^2 + 1)q^4 m_Z^2 \right. \right. \\ \left. \left. - 2(52c_W^4 - 28c_W^2 + 3)q^2 m_Z^4 + (12c_W^4 - 4c_W^2 + 1)m_W^2 (-6q^2 m_Z^2 + 8m_Z^4 + q^4) \right. \right. \\ \left. \left. + (-24c_W^4 + 8c_W^2 - 2)m_Z^6) \right) C_{0WWW}(q^2) + (-6q^2 m_Z^2 + 8m_Z^4 + q^4) (- (1 - 2c_W^2)^2 m_H^2 \right. \\ \left. - 2(12c_W^4 - 4c_W^2 + 1)m_W^2) \right\}, \quad (A7)$$

and

$$A_{ZH}^H(q^2, m_Z^2) = \frac{1}{8q^2(q^2 - 4m_Z^2)^2} \left\{ -2(m_Z^2 - m_H^2)(q^2 - 4m_Z^2) [m_Z^2 B_{0ZZ}(0) - m_H^2 B_{0HH}(0)] \right. \\ \left. + (6m_H^4 (q^2 - m_Z^2) - 9q^2 m_H^2 m_Z^2) B_{0HH}(q^2) + 2(8m_Z^4 (m_H^2 - q^2) - q^2 m_H^4 \right. \\ \left. + 2m_Z^2 (2q^2 m_H^2 - m_H^4 + q^4)) B_{0HZ}(m_Z^2) - (2q^2 m_H^4 + m_Z^2 (3q^2 m_H^2 - 2m_H^4 + 4q^4) \right. \\ \left. - 18q^2 m_Z^4 + 8m_Z^6) B_{0ZZ}(q^2) + m_H^2 \left((-2m_H^4 (q^2 - m_Z^2) - m_H^2 (-2q^2 m_Z^2 + 4m_Z^4 + q^4) \right. \right. \\ \left. \left. - 6q^4 m_Z^2 + 28q^2 m_Z^4 - 16m_Z^6) C_{0ZHZ}(q^2) - 3(2m_H^4 (q^2 - m_Z^2) + m_H^2 (8m_Z^4 - 8q^2 m_Z^2) \right. \right. \\ \left. \left. + q^2 m_Z^2 (2m_Z^2 + q^2)) C_{0HZH}(q^2) \right) + (4m_Z^2 - q^2) (2m_H^2 (q^2 - 4m_Z^2) + 2m_H^4 + q^2 m_Z^2) \right\}. \quad (A8)$$

2. Contributions to the HZZ^* coupling

The corresponding contributions to the HZZ^* coupling can be written as

$$A_{Vf}^Z(p_1^2, m_Z^2, m_H^2) = \frac{1}{(-2m_H^2 (m_Z^2 + p_1^2) + m_H^4 + (m_Z^2 - p_1^2)^2)^2} \left\{ 2[m_H^4 (m_Z^2 + p_1^2) - 2m_H^2 (-4p_1^2 m_Z^2 + m_Z^4 + p_1^4) \right. \\ \left. + (m_Z^2 - p_1^2)^2 (m_Z^2 + p_1^2)] B_{0ff}(m_H^2) + (-2m_Z^2 [4p_1^2 (m_H^2 + m_Z^2) \right. \\ \left. + (m_H^2 - m_Z^2)^2 - 5p_1^4]) B_{0ff}(m_Z^2) + (-2p_1^2 [m_H^2 (4m_Z^2 - 2p_1^2) + m_H^4 + 4p_1^2 m_Z^2 \right. \\ \left. - 5m_Z^4 + p_1^4]) B_{0ff}(p_1^2) + ((m_H^2 - m_Z^2 - p_1^2) [-p_1^4 (-4m_f^2 + 3m_H^2 + m_Z^2) \right. \\ \left. - p_1^2 (8m_f^2 (m_H^2 + m_Z^2) - 10m_H^2 m_Z^2 - 3m_H^4 + m_Z^4) + (m_H^2 - m_Z^2)^2 (4m_f^2 - m_H^2 + m_Z^2) \right. \\ \left. + p_1^6]) C_{0fff}(p_1^2) + 2[-3m_H^4 (m_Z^2 + p_1^2) + m_H^2 (2p_1^2 m_Z^2 + 3m_Z^4 + 3p_1^4) + m_H^6 \right. \\ \left. - (m_Z^2 - p_1^2)^2 (m_Z^2 + p_1^2)] \right\}, \quad (A9)$$

$$\begin{aligned}
A_{Af}^Z(p_1^2, m_Z^2, m_H^2) = & \frac{1}{(-2m_H^2(m_Z^2 + p_1^2) + m_H^4 + (m_Z^2 - p_1^2)^2)^2} \left\{ \left((m_H^2 - m_Z^2 - p_1^2) [-2m_H^2(m_Z^2 + p_1^2) + 4m_H^4 \right. \right. \\
& - 2(m_Z^2 - p_1^2)^2] \Big) B_{0ff}(m_H^2) + \left(-2(m_H^2 - m_Z^2 - p_1^2) [m_H^2(m_Z^2 - 2p_1^2) + m_H^4 + p_1^2 m_Z^2 \right. \\
& - 2m_Z^4 + p_1^4] \Big) B_{0ff}(m_Z^2) + \left(-2(m_H^2 - m_Z^2 - p_1^2) [p_1^2(m_H^2 + m_Z^2) + (m_H^2 - m_Z^2)^2 \right. \\
& - 2p_1^4] \Big) B_{0ff}(p_1^2) + \left((m_H^2 - m_Z^2 - p_1^2) [-p_1^4(-4m_f^2 + m_H^2 + m_Z^2) \right. \\
& - p_1^2(8m_f^2(m_H^2 + m_Z^2) - 6m_H^2 m_Z^2 + m_H^4 + m_Z^4) + (m_H^2 - m_Z^2)^2(4m_f^2 + m_H^2 + m_Z^2) \\
& + p_1^6] \Big) C_{0ff}(p_1^2) + 2[-3m_H^4(m_Z^2 + p_1^2) + m_H^2(2p_1^2 m_Z^2 + 3m_Z^4 + 3p_1^4) + m_H^6 \\
& \left. \left. - (m_Z^2 - p_1^2)^2(m_Z^2 + p_1^2) \right] \right\}, \tag{A10}
\end{aligned}$$

$$\begin{aligned}
A_W^Z(p_1^2, m_Z^2, m_H^2) = & \frac{1}{8(-2m_H^2(m_Z^2 + p_1^2) + m_H^4 + (m_Z^2 - p_1^2)^2)^2} \left\{ \left[-m_H^6((1 - 2c_W^2)^2(m_Z^2 + p_1^2) + 8m_W^2) \right. \right. \\
& - 2m_H^4((12c_W^4 - 4c_W^2 - 7)m_W^2(m_Z^2 + p_1^2) - (1 - 2c_W^2)^2(-4p_1^2 m_Z^2 + m_Z^4 + p_1^4)) \\
& - m_H^2(4m_W^2(16p_1^2 c_W^2(3c_W^2 - 1)m_Z^2 + (-12c_W^4 + 4c_W^2 + 1)m_Z^4 + p_1^4(-12c_W^4 + 4c_W^2 + 1)) \\
& \left. \left. + (1 - 2c_W^2)^2(m_Z^2 - p_1^2)^2(m_Z^2 + p_1^2) - 2(12c_W^4 - 4c_W^2 + 1)m_W^2(m_Z^2 - p_1^2)^2(m_Z^2 + p_1^2) \right] \right. \\
& \times B_{0WW}(m_H^2) + \left[2m_H^4(m_W^2((12c_W^4 - 4c_W^2 - 1)m_Z^2 - 6p_1^2) - (1 - 2c_W^2)^2 m_Z^2(m_Z^2 - 2p_1^2)) \right. \\
& + m_H^2(4m_W^2(8p_1^2 c_W^2(3c_W^2 - 1)m_Z^2 - 2(6c_W^4 - 2c_W^2 + 1)m_Z^4 + 3p_1^4) \\
& + (1 - 2c_W^2)^2 m_Z^2(4p_1^2 m_Z^2 + m_Z^4 - 5p_1^4)) + m_H^6((1 - 2c_W^2)^2 m_Z^2 + 4m_W^2) \\
& \left. \left. + 2m_W^2(m_Z^2 - p_1^2)(p_1^2(60c_W^4 - 20c_W^2 + 1)m_Z^2 + (12c_W^4 - 4c_W^2 + 3)m_Z^4 + 2p_1^4) \right] B_{0WW}(m_Z^2) \right. \\
& + \left[-2m_H^4(m_W^2(p_1^2(-12c_W^4 + 4c_W^2 + 1) + 6m_Z^2) + p_1^2(1 - 2c_W^2)^2(p_1^2 - 2m_Z^2)) \right. \\
& + m_H^2(4m_W^2(8p_1^2 c_W^2(3c_W^2 - 1)m_Z^2 - 2p_1^4(6c_W^4 - 2c_W^2 + 1) + 3m_Z^4) \\
& + p_1^2(1 - 2c_W^2)^2(4p_1^2 m_Z^2 - 5m_Z^4 + p_1^4)) + m_H^6(p_1^2(1 - 2c_W^2)^2 + 4m_W^2) \\
& \left. \left. - 2m_W^2(m_Z^2 - p_1^2)(p_1^2(60c_W^4 - 20c_W^2 + 1)m_Z^2 + p_1^4(12c_W^4 - 4c_W^2 + 3) + 2m_Z^4) \right] B_{0WW}(p_1^2) \right. \\
& + 2 \left[m_H^6(-52c_W^4 - 20c_W^2 - 1)m_W^2(m_Z^2 + p_1^2) - 2p_1^2(1 - 2c_W^2)^2 m_Z^2 \right. \\
& + (-24c_W^4 + 8c_W^2 - 2)m_W^4 + m_H^4(6(12c_W^4 - 4c_W^2 + 1)m_W^4(m_Z^2 + p_1^2) \\
& + m_W^2(2p_1^2(4c_W^4 - 4c_W^2 - 1)m_Z^2 + (84c_W^4 - 36c_W^2 + 3)m_Z^4 + 3p_1^4(28c_W^4 - 12c_W^2 + 1)) \\
& + p_1^2(1 - 2c_W^2)^2 m_Z^2(m_Z^2 + p_1^2)) + m_H^2(-2(12c_W^4 - 4c_W^2 + 1)m_W^4(2p_1^2 m_Z^2 + 3m_Z^4 + 3p_1^4) \\
& - m_W^2(m_Z^2 + p_1^2)(-4p_1^2(36c_W^4 - 16c_W^2 + 3)m_Z^2 + (60c_W^4 - 28c_W^2 + 5)m_Z^4 \\
& + p_1^4(60c_W^4 - 28c_W^2 + 5)) + p_1^2(1 - 2c_W^2)^2 m_Z^2(m_Z^2 - p_1^2)^2 + (12c_W^4 - 4c_W^2 - 1)m_H^8 m_W^2 \\
& \left. \left. + 2m_W^2(m_Z^2 - p_1^2)^2(-p_1^2(1 - 2c_W^2)^2 m_Z^2 + (12c_W^4 - 4c_W^2 + 1)m_W^2(m_Z^2 + p_1^2) \right. \right. \\
& \left. \left. + (8c_W^4 - 4c_W^2 + 1)m_Z^4 + p_1^4(8c_W^4 - 4c_W^2 + 1)) \right] C_{0WW}(p_1^2) - ((1 - 2c_W^2)^2 m_H^2 \right. \\
& \left. + 2(12c_W^4 - 4c_W^2 + 1)m_W^2) (-3m_H^4(m_Z^2 + p_1^2) + m_H^2(2p_1^2 m_Z^2 + 3m_Z^4 + 3p_1^4) + m_H^6 \right. \\
& \left. \left. - (m_Z^2 - p_1^2)^2(m_Z^2 + p_1^2) \right) \right\}, \tag{A11}
\end{aligned}$$

and

$$\begin{aligned}
A_{ZH}^Z(q^2, m_Z^2) = & \frac{1}{16(-2m_H^2(m_Z^2 + p_1^2) + m_H^4 + (m_Z^2 - p_1^2)^2)^2} \left\{ -4(m_H^2 - m_Z^2)(-2m_H^2(m_Z^2 + p_1^2) + m_H^4) \right. \\
& + (m_Z^2 - p_1^2)^2 \left[m_H^2 B_{0HH}(0) - m_Z^2 B_{0ZZ}(0) \right] + 3m_H^2 \left[-m_H^4(7m_Z^2 + 3p_1^2) + 2m_H^2(m_Z^4 - p_1^2 m_Z^2) \right. \\
& + 4m_H^6 + (m_Z^2 - p_1^2)^3 \left. \right] B_{0HH}(m_H^2) + \left[m_H^6(p_1^2 - 11m_Z^2) + 4m_H^4(p_1^2 m_Z^2 + 7m_Z^4 + p_1^4) \right. \\
& - m_H^2(7p_1^2 m_Z^4 + p_1^4 m_Z^2 + 7m_Z^6 + p_1^6) - 4m_H^8 - 2(3m_Z^2 + p_1^2)(m_Z^3 - p_1^2 m_Z)^2 \left. \right] B_{0ZZ}(m_H^2) \\
& - 2 \left[-2m_H^6(m_Z^2 + p_1^2) + m_H^4(6p_1^2 m_Z^2 - 7m_Z^4 + p_1^4) + 2m_H^2 m_Z^2(-9p_1^2 m_Z^2 + 8m_Z^4 + p_1^4) + m_H^8 \right. \\
& + 2p_1^6 m_Z^2 + 6p_1^2 m_Z^6 - 8m_Z^8 \left. \right] B_{0HZ}(m_Z^2) - 2 \left[m_H^6(2p_1^2 - 6m_Z^2) + m_H^4(-11p_1^2 m_Z^2 + 12m_Z^4 - p_1^4) \right. \\
& - 2m_H^2(-3p_1^2 m_Z^4 - 3p_1^4 m_Z^2 + 5m_Z^6 + p_1^6) + m_H^8 + 3m_Z^2(m_Z^2 - p_1^2)(m_Z^2 + p_1^2)^2 \left. \right] B_{0HZ}(p_1^2) \\
& - 6m_H^4 \left[-3m_H^4(2m_Z^2 + p_1^2) + m_H^2(p_1^2 m_Z^2 + 6m_Z^4 + 3p_1^4) + 2m_H^6 - 2(m_Z^2 - p_1^2)^2(m_Z^2 + p_1^2) \right] \\
& \times C_{0HHZ}(p_1^2) - 2 \left[m_H^8(4m_Z^2 - 2p_1^2) - 2m_H^6(11m_Z^4 + p_1^4) + m_H^4(5p_1^2 m_Z^4 - 2p_1^4 m_Z^2 + 12m_Z^6 + p_1^6) \right. \\
& + m_H^2(11m_Z^2 + 5p_1^2)(m_Z^3 - p_1^2 m_Z)^2 + 3m_H^{10} - 2(m_Z^3 - p_1^2 m_Z)^2(p_1^2 m_Z^2 + 4m_Z^4 + p_1^4) \left. \right] C_{0ZZH}(p_1^2) \\
& - 2 \left[-m_H^6(13m_Z^2 + 10p_1^2) + m_H^4(5p_1^2 m_Z^2 + 15m_Z^4 + 8p_1^4) + m_H^2(8p_1^2 m_Z^4 + p_1^4 m_Z^2 - 7m_Z^6 - 2p_1^6) \right. \\
& \left. + 4m_H^8 + m_Z^2(m_Z^2 - p_1^2)^3 \right] \left. \right\}. \tag{A12}
\end{aligned}$$

-
- [1] S. Chatrchyan *et al.* (CMS), Observation of a New Boson at a Mass of 125 GeV with the CMS Experiment at the LHC, *Phys. Lett. B* **716**, 30 (2012), arXiv:1207.7235 [hep-ex].
- [2] G. Aad *et al.* (ATLAS), Observation of a new particle in the search for the Standard Model Higgs boson with the ATLAS detector at the LHC, *Phys. Lett. B* **716**, 1 (2012), arXiv:1207.7214 [hep-ex].
- [3] A. Tumasyan *et al.* (CMS), First evidence for off-shell production of the Higgs boson and measurement of its width, (2022), arXiv:2202.06923 [hep-ex].
- [4] N. Kauer and G. Passarino, Inadequacy of zero-width approximation for a light Higgs boson signal, *JHEP* **08**, 116, arXiv:1206.4803 [hep-ph].
- [5] F. Caola and K. Melnikov, Constraining the Higgs boson width with ZZ production at the LHC, *Phys. Rev. D* **88**, 054024 (2013), arXiv:1307.4935 [hep-ph].
- [6] J. M. Campbell, R. K. Ellis, and C. Williams, Bounding the Higgs Width at the LHC Using Full Analytic Results for $gg \rightarrow e^- e^+ \mu^- \mu^+$, *JHEP* **04**, 060, arXiv:1311.3589 [hep-ph].
- [7] S. Bolognesi, Y. Gao, A. V. Gritsan, K. Melnikov, M. Schulze, N. V. Tran, and A. Whitbeck, On the spin and parity of a single-produced resonance at the LHC, *Phys. Rev. D* **86**, 095031 (2012), arXiv:1208.4018 [hep-ph].
- [8] I. Anderson *et al.*, Constraining Anomalous HVV Interactions at Proton and Lepton Colliders, *Phys. Rev. D* **89**, 035007 (2014), arXiv:1309.4819 [hep-ph].
- [9] B. Şahin, Search for the anomalous ZZH couplings at the CLIC, *Mod. Phys. Lett. A* **34**, 1950299 (2019).
- [10] A. V. Gritsan, J. Roskes, U. Sarica, M. Schulze, M. Xiao, and Y. Zhou, New features in the JHU generator framework: constraining Higgs boson properties from on-shell and off-shell production, *Phys. Rev. D* **102**, 056022 (2020), arXiv:2002.09888 [hep-ph].
- [11] D. Gonçalves, T. Han, S. Ching Iris Leung, and H. Qin, Off-shell Higgs couplings in $H^* \rightarrow ZZ \rightarrow \ell \ell \nu \nu$, *Phys. Lett. B* **817**, 136329 (2021), arXiv:2012.05272 [hep-ph].
- [12] A. Azatov *et al.*, Off-shell Higgs Interpretations Task Force: Models and Effective Field Theories Subgroup Report, (2022), arXiv:2203.02418 [hep-ph].
- [13] P. Sharma and A. Shivaji, Probing non-standard $HVV(V = W, Z)$ couplings in single Higgs production at future electron-proton collider, (2022), arXiv:2207.03862 [hep-ph].
- [14] J. A. Aguilar-Saavedra, A. Bernal, J. A. Casas, and J. M. Moreno, Testing entanglement and Bell inequalities in $H \rightarrow ZZ$, (2022), arXiv:2209.13441 [hep-ph].
- [15] A. T. Nguyen, D. T. Tran, and K. H. Phan, One-loop on-shell and off-shell decay $H^* \rightarrow VV$ at future $e^- e^-$ collider, in *47th Vietnam Conference on Theoretical Physics* (2022) arXiv:2209.13153 [hep-ph].
- [16] B. A. Kniehl, Radiative corrections for associated ZH production at future $e^+ e^-$ colliders, *Z. Phys. C* **55**, 605 (1992).

- [17] K. Hagiwara and M. L. Stong, Probing the scalar sector in $e^+ e^- \rightarrow f \text{ anti-}f H$, *Z. Phys. C* **62**, 99 (1994), arXiv:hep-ph/9309248.
- [18] K. Hagiwara, S. Ishihara, J. Kamoshita, and B. A. Kniehl, Prospects of measuring general Higgs couplings at $e^+ e^-$ linear colliders, *Eur. Phys. J. C* **14**, 457 (2000), arXiv:hep-ph/0002043.
- [19] B. A. Kniehl, Theoretical aspects of standard model Higgs boson physics at a future $e^+ e^-$ linear collider, *Int. J. Mod. Phys. A* **17**, 1457 (2002), arXiv:hep-ph/0112023.
- [20] S. S. Biswal, R. M. Godbole, R. K. Singh, and D. Choudhury, Signatures of anomalous VVH interactions at a linear collider, *Phys. Rev. D* **73**, 035001 (2006), [Erratum: *Phys.Rev.D* **74**, 039904 (2006)], arXiv:hep-ph/0509070.
- [21] D. Choudhury and Mamta, Anomalous Higgs Couplings at an $e \gamma$ Collider, *Phys. Rev. D* **74**, 115019 (2006), arXiv:hep-ph/0608293.
- [22] R. M. Godbole, D. J. Miller, and M. M. Muhlleitner, Aspects of CP violation in the $H ZZ$ coupling at the LHC, *JHEP* **12**, 031, arXiv:0708.0458 [hep-ph].
- [23] S. Dutta, K. Hagiwara, and Y. Matsumoto, Measuring the Higgs-Vector boson Couplings at Linear $e^+ e^-$ Collider, *Phys. Rev. D* **78**, 115016 (2008), arXiv:0808.0477 [hep-ph].
- [24] S. D. Rindani and P. Sharma, Angular distributions as a probe of anomalous ZZH and gammaZH interactions at a linear collider with polarized beams, *Phys. Rev. D* **79**, 075007 (2009), arXiv:0901.2821 [hep-ph].
- [25] I. T. Cakir, O. Cakir, A. Senol, and A. T. Tasci, Probing Anomalous HZZ Couplings at the LHeC, *Mod. Phys. Lett. A* **28**, 1350142 (2013), arXiv:1304.3616 [hep-ph].
- [26] K. Rao, S. D. Rindani, and P. Sarmah, Probing anomalous gauge-Higgs couplings using Z boson polarization at $e^+ e^-$ colliders, *Nucl. Phys. B* **950**, 114840 (2020), arXiv:1904.06663 [hep-ph].
- [27] S. Kumar, P. Poullose, R. Rahaman, and R. K. Singh, Measuring Higgs self-couplings in the presence of VVH and VVHH at the ILC, *Int. J. Mod. Phys. A* **34**, 1950094 (2019), arXiv:1905.06601 [hep-ph].
- [28] K. Rao, S. D. Rindani, and P. Sarmah, Study of anomalous gauge-Higgs couplings using Z boson polarization at LHC, *Nucl. Phys. B* **964**, 115317 (2021), arXiv:2009.00980 [hep-ph].
- [29] L. Chen, G. Heinrich, S. P. Jones, M. Kerner, J. Klappert, and J. Schlenk, ZH production in gluon fusion: two-loop amplitudes with full top quark mass dependence, *JHEP* **03**, 125, arXiv:2011.12325 [hep-ph].
- [30] W. Bizoń, F. Caola, K. Melnikov, and R. Röntsch, Anomalous couplings in associated VH production with Higgs boson decay to massive b quarks at NNLO in QCD, *Phys. Rev. D* **105**, 014023 (2022), arXiv:2106.06328 [hep-ph].
- [31] K. Rao, S. D. Rindani, P. Sarmah, and B. Singh, Polarized Z cross sections in Higgsstrahlung for the determination of anomalous ZZH couplings, (2022), arXiv:2202.10215 [hep-ph].
- [32] P. Bittar and G. Burdman, Form Factors in Higgs Couplings from Physics Beyond the Standard Model, (2022), arXiv:2204.07094 [hep-ph].
- [33] A. V. Gritsan *et al.*, Snowmass White Paper: Prospects of CP-violation measurements with the Higgs boson at future experiments, (2022), arXiv:2205.07715 [hep-ex].
- [34] X. Chen, X. Guan, C.-Q. He, Z. Li, X. Liu, and Y.-Q. Ma, Complete two-loop electroweak corrections to $e^+ e^- \rightarrow HZ$, (2022), arXiv:2209.14953 [hep-ph].
- [35] U. Haisch and G. Koole, Off-shell Higgs production at the LHC as a probe of the trilinear Higgs coupling, *JHEP* **02**, 030, arXiv:2111.12589 [hep-ph].
- [36] C. Englert, Y. Soreq, and M. Spannowsky, Off-Shell Higgs Coupling Measurements in BSM scenarios, *JHEP* **05**, 145, arXiv:1410.5440 [hep-ph].
- [37] A. I. Hernández-Juárez, A. Moyotl, and G. Tavares-Velasco, Bounds on the absorptive parts of the chromomagnetic and chromoelectric dipole moments of the top quark from LHC data, (2021), arXiv:2109.09978 [hep-ph].
- [38] A. I. Hernández-Juárez, A. Moyotl, and G. Tavares-Velasco, New estimate of the chromomagnetic dipole moment of quarks in the standard model, *Eur. Phys. J. Plus* **136**, 262 (2021), arXiv:2009.11955 [hep-ph].
- [39] A. I. Hernández-Juárez, G. Tavares-Velasco, and A. Moyotl, Chromomagnetic and chromoelectric dipole moments of quarks in the reduced 331 model, *Chin. Phys. C* **45**, 113101 (2021), arXiv:2012.09883 [hep-ph].
- [40] A. I. Hernández-Juárez, A. Moyotl, and G. Tavares-Velasco, Contributions to ZZV^* ($V = \gamma, Z, Z'$) couplings from CP violating flavor changing couplings, *Eur. Phys. J. C* **81**, 304 (2021), arXiv:2102.02197 [hep-ph].
- [41] A. I. Hernández-Juárez and G. Tavares-Velasco, Non-diagonal contributions to $Z\gamma V^*$ vertex and bounds on $Z\bar{t}q$ couplings, (2022), arXiv:2203.16819 [hep-ph].
- [42] G. J. Gounaris, J. Layssac, and F. M. Renard, New and standard physics contributions to anomalous Z and gamma selfcouplings, *Phys. Rev. D* **62**, 073013 (2000), arXiv:hep-ph/0003143.
- [43] D. Choudhury, S. Dutta, S. Rakshit, and S. Rindani, Trilinear neutral gauge boson couplings, *Int. J. Mod. Phys. A* **16**, 4891 (2001), arXiv:hep-ph/0011205.
- [44] J. Fleischer and F. Jegerlehner, Radiative Corrections to Higgs Decays in the Extended Weinberg-Salam Model, *Phys. Rev. D* **23**, 2001 (1981).
- [45] B. A. Kniehl, Radiative corrections for $H \rightarrow ZZ$ in the standard model, *Nucl. Phys. B* **352**, 1 (1991).
- [46] K. H. Phan and D. T. Tran, One-loop formulas for off-shell decay $H^* \rightarrow ZZ$ in 't Hooft-Veltman gauge and its applications, (2022), arXiv:2209.12410 [hep-ph].
- [47] S. Kanemura, M. Kikuchi, K. Sakurai, and K. Yagyu, Gauge invariant one-loop corrections to Higgs boson couplings in non-minimal Higgs models, *Phys. Rev. D* **96**, 035014 (2017), arXiv:1705.05399 [hep-ph].
- [48] M. Aoki, S. Kanemura, M. Kikuchi, and K. Yagyu, Radiative corrections to the Higgs boson couplings in the triplet model, *Phys. Rev. D* **87**, 015012 (2013), arXiv:1211.6029 [hep-ph].

- [49] A. Soni and R. M. Xu, Probing CP violation via Higgs decays to four leptons, *Phys. Rev. D* **48**, 5259 (1993), arXiv:hep-ph/9301225.
- [50] Y. Gao, A. V. Gritsan, Z. Guo, K. Melnikov, M. Schulze, and N. V. Tran, Spin Determination of Single-Produced Resonances at Hadron Colliders, *Phys. Rev. D* **81**, 075022 (2010), arXiv:1001.3396 [hep-ph].
- [51] A. M. Sirunyan *et al.* (CMS), Constraints on anomalous Higgs boson couplings using production and decay information in the four-lepton final state, *Phys. Lett. B* **775**, 1 (2017), arXiv:1707.00541 [hep-ex].
- [52] A. M. Sirunyan *et al.* (CMS), Measurements of the Higgs boson width and anomalous HVV couplings from on-shell and off-shell production in the four-lepton final state, *Phys. Rev. D* **99**, 112003 (2019), arXiv:1901.00174 [hep-ex].
- [53] A. M. Sirunyan *et al.* (CMS), Constraints on anomalous Higgs boson couplings to vector bosons and fermions in its production and decay using the four-lepton final state, *Phys. Rev. D* **104**, 052004 (2021), arXiv:2104.12152 [hep-ex].
- [54] V. Khachatryan *et al.* (CMS), Constraints on the spin-parity and anomalous HVV couplings of the Higgs boson in proton collisions at 7 and 8 TeV, *Phys. Rev. D* **92**, 012004 (2015), arXiv:1411.3441 [hep-ex].
- [55] R. Alonso, E. E. Jenkins, A. V. Manohar, and M. Trott, Renormalization Group Evolution of the Standard Model Dimension Six Operators III: Gauge Coupling Dependence and Phenomenology, *JHEP* **04**, 159, arXiv:1312.2014 [hep-ph].
- [56] B. Grzadkowski, M. Iskrzynski, M. Misiak, and J. Rosiek, Dimension-Six Terms in the Standard Model Lagrangian, *JHEP* **10**, 085, arXiv:1008.4884 [hep-ph].
- [57] R. Contino, M. Ghezzi, C. Grojean, M. Muhlleitner, and M. Spira, Effective Lagrangian for a light Higgs-like scalar, *JHEP* **07**, 035, arXiv:1303.3876 [hep-ph].
- [58] D. de Florian *et al.* (LHC Higgs Cross Section Working Group), Handbook of LHC Higgs Cross Sections: 4. Deciphering the Nature of the Higgs Sector **2/2017**, 10.23731/CYRM-2017-002 (2016), arXiv:1610.07922 [hep-ph].
- [59] J. M. Cornwall, Dynamical Mass Generation in Continuum QCD, *Phys. Rev. D* **26**, 1453 (1982).
- [60] J. Papavassiliou, On the connection between the pinch technique and the background field method, *Phys. Rev. D* **51**, 856 (1995), arXiv:hep-ph/9410385.
- [61] S. Hashimoto, J. Kodaira, Y. Yasui, and K. Sasaki, The Background field method: Alternative way of deriving the pinch technique's results, *Phys. Rev. D* **50**, 7066 (1994), arXiv:hep-ph/9406271.
- [62] T. Hahn, Generating Feynman diagrams and amplitudes with FeynArts 3, *Comput. Phys. Commun.* **140**, 418 (2001), arXiv:hep-ph/0012260.
- [63] R. Mertig, M. Bohm, and A. Denner, FEYN CALC: Computer algebraic calculation of Feynman amplitudes, *Comput. Phys. Commun.* **64**, 345 (1991).
- [64] V. Shtabovenko, R. Mertig, and F. Orellana, New Developments in FeynCalc 9.0, *Comput. Phys. Commun.* **207**, 432 (2016), arXiv:1601.01167 [hep-ph].
- [65] V. Shtabovenko, R. Mertig, and F. Orellana, FeynCalc 9.3: New features and improvements, *Comput. Phys. Commun.* **256**, 107478 (2020), arXiv:2001.04407 [hep-ph].
- [66] T. Hahn and M. Perez-Victoria, Automated one loop calculations in four-dimensions and D-dimensions, *Comput. Phys. Commun.* **118**, 153 (1999), arXiv:hep-ph/9807565.
- [67] A. Denner, S. Dittmaier, and L. Hofer, Collier: a fortran-based Complex One-Loop Library in Extended Regularizations, *Comput. Phys. Commun.* **212**, 220 (2017), arXiv:1604.06792 [hep-ph].
- [68] A. I. Hernández-Juárez, Mathematica code for hzz analysis, <https://gitlab.com/fcfm-buap-rc-group/zzh-anomalous-couplings>, accessed: 2022-11-22.
- [69] C. Degrande, N. Greiner, W. Kilian, O. Mattelaer, H. Mebane, T. Stelzer, S. Willenbrock, and C. Zhang, Effective Field Theory: A Modern Approach to Anomalous Couplings, *Annals Phys.* **335**, 21 (2013), arXiv:1205.4231 [hep-ph].
- [70] S. Gorla, G. Passarino, and D. Rosco, The Higgs Boson Lineshape, *Nucl. Phys. B* **864**, 530 (2012), arXiv:1112.5517 [hep-ph].
- [71] E. Maina, Vector boson polarizations in the decay of the Standard Model Higgs, *Phys. Lett. B* **818**, 136360 (2021), arXiv:2007.12080 [hep-ph].
- [72] E. Maina and G. Pelliccioli, Polarized Z bosons from the decay of a Higgs boson produced in association with two jets at the LHC, *Eur. Phys. J. C* **81**, 989 (2021), arXiv:2105.07972 [hep-ph].
- [73] G. Buchalla, O. Cata, and G. D'Ambrosio, Nonstandard Higgs couplings from angular distributions in $h \rightarrow Z\ell^+\ell^-$, *Eur. Phys. J. C* **74**, 2798 (2014), arXiv:1310.2574 [hep-ph].
- [74] S. Berge, S. Groote, J. G. Körner, and L. Kaldamäe, Lepton-mass effects in the decays $H \rightarrow ZZ^* \rightarrow \ell^+\ell^-\tau^+\tau^-$ and $H \rightarrow WW^* \rightarrow \ell\nu\tau\nu_\tau$, *Phys. Rev. D* **92**, 033001 (2015), arXiv:1505.06568 [hep-ph].
- [75] H.-R. He, X. Wan, and Y.-K. Wang, Anomalous $H \rightarrow ZZ \rightarrow 4\ell$ decay and its interference effects on gluon-gluon contribution at the LHC, *Chin. Phys. C* **44**, 123101 (2020), arXiv:1902.04756 [hep-ph].